POWER SPECTRA AND COSPECTRA FOR WIND AND SCALARS IN A DISTURBED SURFACE LAYER AT THE BASE OF AN ADVECTIVE INVERSION

K. G. MCNAUGHTON[1,*] and J. LAUBACH[2]
[1]*Station de Bioclimatologie – INRA, B.P. 81, 33883 Villenave d'Ornon cedex, France;*
[2]*Max-Planck-Institut für Biogeochemie, Postfach 10 01 64, D-07701 Jena, Germany*

(Received in final form 14 October 1999)

Abstract. This paper reports power spectra and cospectra of wind speed and several scalars measured at two heights near the base of an advective inversion. The inversion had formed over a paddy field downwind of an extensive dry region. Winds over the paddy field were variable in strength and direction, as a result of convective motions in the atmospheric boundary layer passing over from the dry region upwind. Fetch over the rice was large enough that advective effects on the transport processes were small at the upper level and negligible at the lower level. Results from the lower level are interpreted in terms of a horizontally homogeneous, but disturbed, surface layer.

Power spectra of longitudinal and lateral velocity were substantially enhanced at low frequencies. The resulting vertical motions added only a small amount to the spectrum of vertical velocity but this strongly affected scalar power spectra and cospectra. These were all substantially enhanced over a range of low frequencies. We also found that differences in lower boundary conditions cause differences among scalar spectra at low frequencies.

Our analysis shows that the spectra and cospectra have three components, characterized by different scaling regimes. We call these the ILS (inner-layer scaling), OLS (outer-layer scaling) and CS (combined scaling) components. Of these, the CS component had not previously been identified. We identify CS components of spectra by their independence of height and frequency. Spectra with these characteristics had been predicted by Kader and Yaglom for a layer of the atmosphere where spectral matching between ILS and OLS was proposed. However, we find that the velocity and scalar scales used by Kader and Yaglom do not fit our results and that their concept of a matching layer is incompatible with our application. An alternative basis for this behaviour and alternative scales are proposed.

We compare our decomposition of spectra into ILS, CS and OLS components with an extended form of Townsend's hypothesis, in which wind and scalar fluctuations are divided into 'active' and 'inactive' components. We find the schemes are compatible if we identify all OLS spectral components as inactive, and all CS and ILS components as active.

By extending the implications of our results to ordinary unstable daytime conditions, we predict that classical Monin–Obukhov similarity theory should be modified. We find that the height of the convective boundary layer is an important parameter when describing transport processes near the ground, and that the scalar scale in the ILS part of the spectrum, which includes the inertial subrange, is proportional to observation height times the local mean scalar gradient, and not the Monin–Obukhov scalar scale parameter. The former depends on two stability parameters: the Monin–Obukhov stability parameter and the ratio of the inner-layer and outer-layer velocity scales. The outer-layer scale can reflect disturbances by topographically-induced eddying as well as by convective motions.

* E-mail: mcnaught@bordeaux.inra.fr

Boundary-Layer Meteorology **96:** 143–185, 2000.
© 2000 *Kluwer Academic Publishers. Printed in the Netherlands.*

Keywords: Unsteadiness, Scalar transport, Townsend's hypothesis, Active and inactive turbulence, Advection, Monin–Obukhov similarity theory.

1. Introduction

This paper is one of several based on an experiment at Warrawidgee, New South Wales, Australia (McNaughton and Laubach, 1998; Laubach and McNaughton, 1998; Laubach et al., 2000). It investigates the effects of slow wind variations on scalar transport processes near the ground. These variations are identified with the concept of inactive turbulence, which was first proposed by Townsend (1961) in the context of momentum transport. Townsend noted that 'turbulent intensities in constant-stress layers vary considerably between different flows of the same stress', and he observed 'it is difficult to reconcile these observations without supposing that the motion at any point consists of two components, an active component responsible for turbulent transfer and determined by the stress distribution and an inactive component which does not transfer momentum or interact with the universal component'. This proposal is now known as 'Townsend's hypothesis'. It has been supported by Bradshaw (1967) and others using results from wind tunnels (for a review see Raupach et al., 1991) and, more recently, by Högström (1990), Katul and Chu (1998) and Katul et al. (1996, 1998) using results from the atmospheric surface layer.

The papers just cited dealt principally with momentum transport, though some of them also reported temperature power spectra and velocity-temperature cospectra. The principal focus of our research is on scalar transport, so we measured fluctuations of other scalars besides temperature in our experiment. These were carbon dioxide concentration, c, specific humidity, q, and temperature, T. From these we also calculated two composite scalars, equivalent temperature, α, and saturation deficit, d. These were chosen to represent a range of surface controls over the release of the scalar substance, which is to say, a range of lower boundary conditions. This allows us to examine the role of lower boundary conditions on scalar transport.

The initial idea for this research came from an 'advection' experiment carried out over irrigated grass on the Crau plain in France (de Bruin et al., 1991). During that experiment measurements were made of the temperature profile at six levels above irrigated grass in an advective situation. An example of these results is shown as Figure 1 (Leo Kroon, personal communication, 1992). What is striking about these results is that all levels of the temperature profile rise and fall in a co-ordinated fashion while the profile as a whole generally retains its shape. When we first looked at these data we thought the likely explanation was that the profile was affected by slow variations in wind speed. We reasoned that such variations would have caused short-term variations in friction velocity and corresponding variations in the temperature gradient in the surface layer. It was expected that the observed

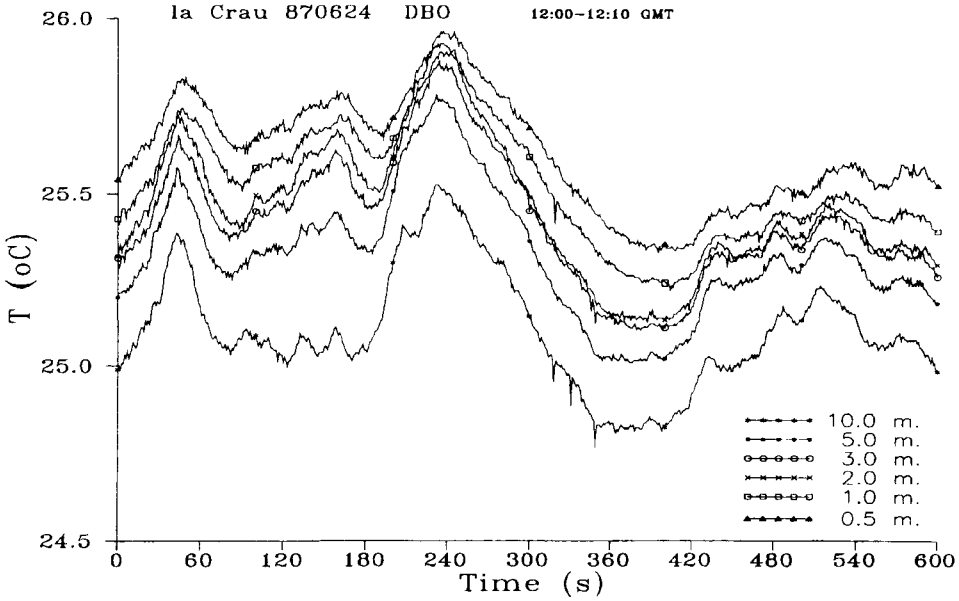

Figure 1. Temperature profiles over irrigated grass on the La Crau plain in June 1987. These temperatures were measured at 47 m downwind from the boundary onto dry land. The sensors probably had a time constant of about 15 s, thus filtering out most fluctuations at frequencies higher than 0.1 Hz. The temperature profile tends to maintain its shape despite the variations affecting all levels (courtesy of de Bruin and Kroon, 1992).

variations would have extended downwards into the crop and so would have caused changes in leaf temperature. That is, we interpreted these data as suggesting that temperature conditions within the canopy were unsteady.

The temperature variations shown in Figure 1 are only about 0.5 °C. Presumably the humidity profile varied in a similar way but with larger amplitude. Together, we argued, the effect of these would have been quite large variations in saturation deficit within the grass canopy. This led to the interesting speculation that the transpiration flux, and so the energy balance of the crop, also varied significantly at the ground in step with changes in the overhead wind speed. From this we reasoned that unsteadiness of the wind could modify transport processes near the ground by causing the largest fluxes to occur during intervals of largest wind speed and most vigorous turbulence. Further, we reasoned that this modification would be most significant for scalar fluxes that were most sensitive to changes in surface concentration, and hence wind speed. That is to say, differences in lower boundary conditions would cause differences in scalar transport processes. Testing this proposition was the task we set ourselves in our experiment at Warrawidgee.

Our earlier papers show that we have made good progress towards demonstrating the truth of these deductions. McNaughton and Laubach (1998) showed that the surface fluxes of temperature and humidity do indeed vary in step with

low-frequency variations in the wind at Warrawidgee, and a theoretical treatment showed that this would affect the values of the eddy diffusivities for temperature, K_T, and humidity, K_q, differently. They predicted that, for conditions like those at Warrawidgee, the ratio K_T/K_q should be increased by about 10% above the value of one predicted by Monin–Obukhov similarity theory. This estimate agreed well with the average experimental value of $K_T/K_q = 1.10$ (Laubach et al., 2000).

Yet there are concerns. Our theoretical treatment extended Townsend's ideas of active and inactive fluctuations of wind components to scalars. This extension has never been examined experimentally, so the basis of our theory remains speculative. Also, the values of K_T/K_q found at Warrawidgee disagree sharply with the K_T/K_q values of about 0.7 found by Lang et al. (1983) in an earlier experiment over a similar paddy field at a nearby site, though the two experiments agree very well in other respects. We suggest that experimental error in the earlier work explains the disagreement (Laubach et al., 2000), but such retrospective assessment can never be absolutely secure. A subsidiary aim of the present work, then, is to check consistency of our results by examining our measured scalar spectra and cospectra over a range of scalars.

2. Experimental

A fuller description of the Warrawidgee site and instrumentation is given by Laubach et al. (2000). Here we emphasize the experimental criteria used when selecting the Warrawidgee site and choosing the instrumentation.

2.1. Site selection

In choosing our experimental site we wanted one where unsteady winds would cause large swings in surface temperature and humidity, and we wanted the evaporation rate to respond sensitively to those swings. We also wished to make our measurements in near-ideal conditions where we could reasonably expect all scalar statistics to obey Monin–Obukhov similarity, in the absence of the effects of unsteadiness.

We chose a site in a paddy field on the western edge of an irrigation area, with extensive dry rangelands to the west, and beyond that the dry grasslands of the Hay plain. Convective motions in the atmospheric boundary layer over this dry region would, we expected, produce variable winds at the experimental site.

The strong dry-to-wet contrast was chosen because this would create large vertical gradients in saturation deficit, so variations in wind speed would produce large changes in saturation deficit within the crop. Also, with water freely available to the rice crop, the evaporation rate would be sensitive to such variations. That is, we chose an advective situation not because it was advective *per se*, but because it provided the right combination of steep profiles of saturation deficit, low surface resistance and variable winds overhead.

The final requirement was that we wanted conditions where Monin–Obukhov similarity might be expected to apply were the wind steady. We therefore sought a large flat field with as large a fetch as possible. That is, we tried to minimize the significance of horizontal gradients and vertical flux divergence: these are complications in our work that we would rather have avoided completely. The site chosen at Warrawidgee was close to ideal in this respect.

2.2. INSTRUMENTATION

Our instrumentation was fairly conventional, with fast-response sensors for wind and scalars, and gradient-measuring equipment for scalars at two levels, 2.0 m and 3.9 m above the displacement height of the rice crop. The 2.0 m height was set at about three times crop height above the displacement height, to ensure the measurements were made above the roughness sub-layer (Kaimal and Finnigan, 1994) while maintaining the maximum possible fetch-to-height ratios for winds from westerly directions. For the chosen heights these ratios were about 200 : 1 and 100 : 1 for the lower and upper level, respectively, though this varied somewhat with wind direction, even within runs. Details are given by Laubach et al. (2000).

We used CSAT-3 sonic anemometers (Campbell Scientific, Logan, UT) to measure wind, and fast thermocouples from the same source to measure temperature fluctuations. For specific humidity and concentration of carbon dioxide we used open-path infra-red gas analysers (IRGA) constructed to the design of Auble and Meyers (1992). These rapid sensors provided time series at 10 Hz, which allowed computation of the various fluxes, power spectra and cospectra reported below.

We also measured the remaining components of the one-dimensional energy budget of the field. These were to cross-check our measurements of the convective energy fluxes and to allow calculation of the surface resistance by inverting the Penman–Monteith equation. We measured net radiation at 7 m above ground level, and placed two heat flux plates at the surface of the mineral soil in the paddy. Water depth and temperature were recorded to allow calculation of energy storage in the water layer.

We placed an aspirated probe for temperature and humidity within the crop to record the changing conditions there. The sensor was placed at 2/3 of crop height above water level (Humitter 50 Y, Vaisala, Helsinki, Finland). We monitored crop ‘surface’ temperature with an infra-red thermometer (Model KT-15, Heitronics, Wiesbaden, Germany); this viewed a target area of about 0.45 m diameter. No attempt was made to measure conditions upwind of the paddy or the horizontal gradients over the paddy.

2.3. DATA PROCESSING

2.3.1. *Calculation of Spectra*

We used the LabVIEW (National Instruments, Austin, TX) software package for data collection and processing. Power spectra and cospectra were calculated using the complex Fast Fourier Transform (FFT) available in this package. Since this FFT software does not require that the number of data be a power of two, we could use the full length of our data runs. In our experiment, data were recorded at 10 Hz during runs of 20 min, giving records of 12000 points for all 'fast' measurements at 2.0 and 3.9 m. We collected other data, such as surface infrared temperature and within-canopy temperature and humidity, at 1 Hz, so spectra for these variables are calculated using 1200 data points.

Before employing the FFT algorithm the data series were conditioned following common procedures in micrometeorology: linear trends were removed and the series multiplied by a Hamming window ('tapering'), after which the mean of the tapered series was removed. A discussion of the effects of these procedures can be found in Kaimal and Finnigan (1994).

For each run and each fast (slow) sensor, the FFT algorithm produced a set of 6000 (600) complex spectral coefficients (discarding the redundant 'negative harmonics'), the last of them representing the spectral energy at the Nyquist frequency (5 Hz), the first representing the spectral energy at the inverse of the sampling rate. Their real parts and imaginary parts were combined in the usual way to give power spectra, cospectra, and quadrature spectra (e.g., Stull 1988, p. 330–331). The resulting spectra were then smoothed as follows. The first 20 coefficients were subjected to an overlapping block average of width 3 points. This reduced the most erratic variations at the statistically unreliable low-frequency end. All other coefficients were averaged into non-overlapping classes of logarithmically increasing width (so that they appear equidistant on a logarithmic frequency axis). It was enforced that the smoothing procedure preserved total variance or covariance, with each smoothed spectrum consisting of 57 (42) coefficients.

2.3.2. *Averaging of Spectra*

The results from our spectral analysis are presented as averages over 31 runs. The individual spectra were scaled before averaging, using the scaling parameters indicated in the figures by the labels on either axis. For this the friction velocity, u_* and the scalar scale, s_*, were always taken at the lower level, 2.0 m. Scaling the ordinate before averaging means that the shapes of the individual spectra all have equal influence on the shape of the averaged spectrum, rather than the average being dominated by those spectra with the largest amplitudes. On the abscissa the spectra were averaged either at matching natural frequencies or at matching normalized frequencies, fz/u, where z is height and u is streamwise wind velocity, as indicated by the abscissa label.

2.3.3. *Separation Correction*

The IRGA paths were located on the same levels as the paths of the sonic anemometers, and about 0.3 m distant from them. The only novelty in our arrangement was that we placed the fast thermocouple between the measurement paths of the IRGA and the sonic anemometer, about 0.05 m distant from the IRGA path. This was to facilitate comparisons between scalars. Laubach and McNaughton (1998) discuss procedures to correct for sensor separation with this arrangement of sensors. Such corrections are important when calculating fluxes, so vertical cospectra have been corrected using the transfer function for sensor separation as described by Moore (1986). Corrections to the horizontal cospectra are insignificant because the bulk of the covariance is at frequencies lower than those affected by sensor separation.

2.4. DATA SELECTION

The Warrawidgee experiment ran from January 19 to February 9, 1997. Of the daytime runs recorded during this time 42 runs, each of 20 min duration, were judged suitable for further analysis (Laubach et al., 2000). This set included all runs when the wind was reliably from across the paddy field, with mean fetch exceeding 400 m.

From these runs we further selected 31 runs, excluding cases where mean wind speed at 2.0 m exceeded 5 m s^{-1} or net radiation was less than 100 W m^{-2}. This selection was made to remove those cases in which aliasing errors were large due to high wind speed, and cases where the total heat flux was small. It was expected that this procedure would also select for more strongly convective situations upwind. In the event, the various power spectra and cospectra of the removed 11 runs were very similar in character to those reported here, apart from small differences at high frequencies due to aliasing.

Net radiation varied somewhat during many of the runs. We found no systematic differences in power spectra and cospectra between periods with steady net radiation and the average from the 31 periods reported here.

Conditions were stable at both levels on the instrument tower in all these runs, with Obukhov lengths ranging from 9 m to 65 m, as determined from measurements at 2.0 m.

3. Theory

The first part of this section analyses differences in the boundary conditions that govern release of various scalars at the ground. This sets the scene for interpreting observed differences between the scalar power spectra and the scalar flux cospectra at low frequencies. Also, as we will show, it provides a means of identifying the ‘outer-layer scaling’ component of our scalar spectra and cospectra (defined

below). The second part of the theory is concerned with the development of scaling laws for spectra. We adapt theory that Kader and Yaglom (1991) (henceforth KY91) have developed for a mixed convection sub-layer within the surface layer, lying between layers of purely forced and purely free convection. We use their results to identify components of spectra at a single level. This theory is reassessed later in the paper, after the experimental results have been presented.

Throughout the paper we define vertical fluxes of scalars by $F_s = \overline{w's'}$, where w is vertical wind speed, s is scalar concentration, and overbars and primes signify an average over a run and deviations from that average, respectively. Similarly, horizontal fluxes are given by $\overline{u's'}$ where u is horizontal wind speed in the direction of the mean wind.

3.1. BOUNDARY CONDITIONS FOR SCALARS

Scalar power spectra often vary from one scalar species to another, and they often show enhanced variance at low frequencies when compared with the classic Kansas spectrum (Kaimal et al., 1972). These features are associated with enhanced velocity fluctuations at low frequency and are usually attributed to origins outside the surface layer. For example, Andreas (1987) observed enhanced variance of temperature and humidity at low frequencies over snow and suggested that 'large-scale, topographically-induced velocity fluctuations simply advect the embedded scalar field, giving it spectral characteristics similar to the longitudinal velocity spectrum'. Similarly, de Bruin et al. (1993) proposed that the elevated humidity variances they observed near the ground were affected by the humidity fluctuations embedded in the convective boundary layer, overhead. While explanations such as these are no doubt correct in some cases, remote sources of scalar variance do not appear to have significantly affected our results at Warrawidgee.

Two of the three scalar species we measured directly at Warrawidgee, CO_2 concentration, c, and specific humidity, q, had almost zero flux over the parched upwind plain, so the air above the internal boundary layer (IBL) over our field exhibited neither flux, fluctuation nor gradient in c or q. This was observed directly on days with easterly winds when fetch was very short so that air came directly onto our upper sensors without interacting with the rice paddy. We can state with certainty therefore that the c and q variances observed in our experiment were generated wholly by processes acting within the IBL over the rice. There was some temperature variance above the IBL, but this had small affect on our results.

Since 'advected variance' had little effect on our results, and since all scalars over our field were transported by the same velocity field, the main differences in scalar spectra must have had their origin in differences in scalar sources at the ground. Such effects are of central interest to our investigation because our earlier theory (McNaughton and Laubach, 1998) was constructed on the assumption that scalar source strengths are linked to 'inactive' variations in wind speed, and we hope to identify 'inactive' turbulence by these differences.

We present here a simple analysis of how a transpiring crop defines different lower boundary conditions for different scalar species.

3.1.1. *Types of Lower Boundary Conditions*

Lower boundary conditions for scalars can be of many types, though three will suffice for the discussion here. The simplest of these are the extreme types: the 'constant-concentration' and 'constant-flux' boundary conditions. As their names suggest, these take the forms $z = 0$: $s = s_0$ and $z = 0$: $F_s = F_{s,0}$, respectively, where s_0, the surface concentration of scalar, and $F_{s,0}$, the flux of scalar at the surface, are both constants, which is to say, independent of the surface concentrations of any scalar. Good examples of constant-concentration boundary conditions are $z = 0$: $T = 0$ °C and $q = 3.8 \times 10^{-3}$ kg kg^{-1} for temperature and humidity at the surface of a field of melting snow or ice, and $z = 0$: $d = 0$, for the saturation deficit, d, at a wet surface. Good examples of constant-flux boundary conditions are those describing the efflux of trace gases, such as radon or CH_4, from soil where the rate of generation does not depend on the fluctuating meteorological conditions and minor changes in surface concentrations. Nearly as good an example is the boundary condition describing the uptake of CO_2 by a photosynthesizing crop, since photosynthesis is principally controlled by receipt of shortwave radiation and varies little with typical short-term changes in CO_2concentration in a canopy. Taking the lower boundary condition for CO_2 to be a constant-flux boundary condition, we write

$$z = 0 : \frac{\mathrm{d}F_c}{\mathrm{d}c} = 0, \tag{1}$$

where $\mathrm{d}F_c/\mathrm{d}c$ has units of m s^{-1}. Linking the constant-flux and constant-concentration extremes is a more general type of boundary condition, called a 'radiation' boundary condition. This type takes the form

$$z = 0 : k_1 F_s + k_2 s = 1, \tag{2}$$

where k_1 and k_2 are constants. It is so named because it can be used to describe heat exchange from a heated object that cools by (linearized) emission of thermal radiation (Carslaw and Jaeger, 1950). Equation (2) links changes in surface flux to any changes in surface concentration caused by some external action, such as a change in wind speed. The ratio of these is $\mathrm{d}F_s/\mathrm{d}s = -k_2/k_1$. The boundary condition (2) becomes more like a constant-concentration boundary condition as $k_2/k_1 \to \pm\infty$, and more like a constant-flux boundary condition as $k_2/k_1 \to 0$.

3.1.2. *Sensitivity of Equivalent Temperature and Saturation Deficit Fluxes to Surface Concentrations*

Of course, not all boundary conditions are of these simple kinds. For example, the fluxes of temperature and humidity, F_T and F_q, obey the energy balance constraint

$$z = 0 : \rho c_p F_T + \rho\lambda F_q = R_n - G, \tag{3}$$

where ρ is the density of air, c_p is the specific heat of air at constant pressure, λ is the latent heat of vaporization of water and R_n is the net radiation. This boundary condition has the complicating features that it couples the behaviour of two scalar fluxes, so it is insufficient to define the behaviour of either one individually.

We can address this problem by introducing a second boundary condition, which also connects the scalars T and q. We write this as the big-leaf canopy model equation

$$z = 0 : F_q = \frac{d}{r_s}, \tag{4}$$

where r_s is the surface resistance, and the saturation deficit, d, depends on both temperature and humidity. In principle then, Equations (3) and (4) are sufficient to define the behaviour of both T and q at the surface, but each equation still links two scalars and the relationship with d is non-linear.

McNaughton (1976) described a way to simplify this situation. There are two steps. The first is to linearize the saturation deficit and the second is to manipulate the resulting equations to produce a pair of equations, each in terms of the flux and concentration of a single scalar species. Full details may be found in the original paper. Here we present only a few features that are relevant to our present work.

Linearization of the saturation deficit gives

$$d = q^*(\overline{T_0}) + \frac{c_p}{\lambda}\epsilon(\overline{T_0})(T - \overline{T_0}) - q, \tag{5}$$

where ϵ is λ/c_p times the slope of the saturation specific humidity-temperature relationship $\mathrm{d}q^*(T)/\mathrm{d}T$ at $T = \overline{T_0}$. For our second scalar variable we define α to be the equivalent temperature, which we write as

$$\alpha = T + \frac{\lambda}{c_p}q. \tag{6}$$

Notice that the variables α and d, as defined here, are essentially the same as in McNaughton and Laubach (1998), but in different units. What is called α here was $\alpha/\rho c_p$ there, and what is called d here was $d/\rho\lambda$ there. Next, we define the associated fluxes of equivalent temperature, F_α, and saturation deficit, F_d. They allow us to write a pair of independent boundary conditions for these two variables. These are

$$z = 0 : F_d + \frac{1+\epsilon}{r_s}d = \epsilon\frac{R_n - G}{\rho\lambda} \tag{7}$$

and

$$z = 0 : F_\alpha = \frac{R_n - G}{\rho c_p}. \tag{8}$$

The boundary condition (7) is of the radiation type. In the present case ($\epsilon \approx 3$ and $r_s \approx 30$ s m^{-1}) this will behave rather like a constant-concentration condition. (In the limit of $r_s = 0$ we would have $d = 0$.) Equation (8) is a constant-flux type of boundary condition. We expect CO_2 assimilation by the crop to be governed by an equation of the same form, so then we have $\mathrm{d}F_d/\mathrm{d}d < \mathrm{d}F_\alpha/\mathrm{d}\alpha = \mathrm{d}F_c/\mathrm{d}c$.

Implicit in this simple argument is the assumption that net radiation and the heat storage flux are independent of surface temperature. This is not quite true. Unfortunately, allowance for it would require a full analysis of the energy balance of the surface. Rather than do that here, we simply note that a dependence of (R_n - G) on surface temperature will cause F_α to vary somewhat with α at the surface, so F_α will behave somewhat less like a constant-flux variable than will c. Qualitatively then, we predict that a more realistic representation of the sequence of sensitivities should be $\mathrm{d}F_d/\mathrm{d}d < \mathrm{d}F_\alpha/\mathrm{d}\alpha < \mathrm{d}F_c/\mathrm{d}c$.

The scalars T and q cannot be generally placed in the above list because their positions depend on the conditions of the experiment. Even then, they could only be found from a rather more detailed analysis of the surface energy budget than has been attempted here. For this reason we present our spectral results in terms of α and d, to take advantage of the predictability of these scalars, as well as in terms of the directly observed variables T and q.

In our experiment, 'inactive' changes in wind speed tended to cause changes in surface fluxes (McNaughton and Laubach, 1998). This was so because short-term changes in wind speed produced short-term changes in eddy diffusivities, tending to change gradients near the ground and alter absolute concentrations at the ground. For d, the analysis above shows that this tendency would cause changes in surface flux that would oppose the original action, tending to increase the (downward) flux and therefore the gradient at just those moments when the original action of the wind is to decrease it, and vice versa. There would be no such reaction by F_c, so gradients and surface concentration would vary without negative feedback. That is, our analysis predicts the sequence $\sigma_c/c_* > \sigma_\alpha/\alpha_* > \sigma_d/d_*$ for the standard deviations of concentration of these variables. This should be evident in the parts of their spectra influenced by 'inactive' variations of the wind.

3.2. Scaling relationships for spectra

In our earlier theoretical work (McNaughton and Laubach, 1998) we assumed that velocity and scalar fluctuations could all be divided into active and inactive parts, thus

$$a = \bar{\alpha} + a'_p + a'_a, \tag{9}$$

where a is any scalar or velocity component, the primes indicate fluctuations and the subscripts 'a' and 'p' indicate active and inactive parts, respectively. The inactive fluctuations were associated with the time scale of the convective processes in the convective boundary layer overhead, while the time scale of the active fluctuations was identified with the surface layer time scale, z/u_*. If the power spectra of active and inactive components are separated by a spectral gap there is no interaction between active and inactive components, their frequency ranges being separate, so $\overline{a'_a b'_p} = 0$, where a and b are any fluctuating quantities.

Most of the power spectra observed at Warrawidgee show variance spread over a wide range of frequencies, without any obvious spectral gaps, as will be shown below. Indeed, just where the simple conceptual model proposes a spectral gap we find that scalar spectra follow a -1 power law. Segments of u spectra with -1 power laws are well known in flows in channels and wind tunnels, but their existence in the atmosphere was doubted (Raupach et al., 1991). Recently a number of new atmospheric examples have been reported (KY91; Katul et al., 1998; Katul and Chu, 1998). Raupach et al. (1991) and KY91 regard this -1 power-law behaviour as the signature of a matching layer between a layer dominated by large-scale motions above and a layer dominated by small-scale shear-produced motions near the surface. Turbulence of this intermediate kind was not considered by McNaughton and Laubach (1998) when proposing the simple conceptual division embodied in Equation (9).

If this behaviour does represent an interaction between large and small-scale processes, then it is likely that our power spectra have three parts: at the highest frequencies is a part that must observe the scaling relationships of the 'inner layer' and that must be active in carrying flux; at the lowest frequencies is a part that must observe the scaling relationships of the 'outer layer' – in our case those of the convective boundary layer (CBL) overhead – and be inactive in carrying flux because in very large-scale motions the wind moves horizontally near the ground; and at intermediate frequencies is a part that results from the interaction of the 'inner' and 'outer' motions and that observes both types of scaling simultaneously. We have yet to establish whether an interaction of this nature occurs, and if so whether the resulting turbulence transports scalars.

The following treatment relies heavily on the dimensional arguments of KY91, whose analysis was applied to layers of the atmosphere. They propose 'three special sublayers that have self-preserving turbulence structures'. In the lowest layer friction dominates and buoyancy can be ignored. In the highest layer buoyancy dominates and friction can be ignored, while in the middle layer the turbulent motions reflect the effects of both friction and buoyancy. The middle layer is assumed to be a matching layer between the inner-layer and outer-layer regimes. This treatment does not recognise regional-scale processes, so it deals with only one velocity scale, u_* and only one scalar scale, s_*.

We will analyse spectra that are influenced by both local and regional-scale processes. Therefore, we attempt to follow the treatment of KY91 while maintaining a

distinction between local and regional scales. This is not altogether successful and we point out some problems. Even so, the results obtained have very substantial heuristic value because they do predict features that we will observe in the experimental results. As befits our changed focus, we use terminology related to scaling regimes rather than atmospheric layers when referring to spectral behaviour. We choose to work in the frequency domain because our application is to time series made by fixed sensors.

3.2.1. *Inner-Layer Scaling (ILS)*

Inner-layer scaling (ILS) is appropriate to parts of the spectrum dominated by the effects of friction with the ground. Here we suppose that turbulence processes can be described in terms of the similarity parameters z, u_* and s_*. In fact, each transported scalar has associated with it a concentration scale, s_* so there are a series of such parameters, one for each scalar. Therefore, the ILS frequency scale must be z/u_* and the various spectra and cospectra of velocity and scalar components must take the form

$$fC_{i,j}(f) = \chi_*^i \chi_*^j \psi_{i,j}\left(\frac{fz}{u}\right), \tag{10}$$

where z_0 is the roughness length of the surface, i, j = 1, 2, 3, 4 indicate wind components u, v, w and s respectively, and $\chi_*^1 = \chi_*^2 = \chi_*^3 = u_*$ and $-\chi_*^4 = F_{s,0}/u_* = s_*$, where s indicates any chosen scalar. $C_{i,j}$ is the power spectrum when $i = j$ and the cospectrum when $i \neq j$. The functions $\psi_{i,j}(fz/u)$ are distinct universal functions for each selection of i and j, but independent of the particular choice of scalar. Henceforth, we will refer to $C_{i,j}$ as the spectrum, being a power spectrum or cospectrum according to whether the indices are equal or not. The universal functions $\psi_{i,j}(fz/u)$ are known empirically from the neutral runs at Kansas (Kaimal et al., 1972).

Equation (10) expresses inner-layer scaling (ILS) of the spectrum. It states that, if turbulence measurements be made at two heights in the inner layer and a spectrum from each level be plotted against natural frequency, then $fC_{i,j}$ from the two heights will have the same shape and amplitude, but will be displaced horizontally along the frequency axis, as shown in Figure 2a.

3.2.2. *Outer-Layer Scaling (OLS)*

In the outer layer, by contrast, the appropriate frequency scale depends on the turbulence length and velocity scales that characterize the OLS motions, so it does not change with height. For our situation, where the outer layer is the convective planetary boundary layer, the length scale is the height of the inversion base at the top of the CBL, z_i, and the velocity scale is the convective velocity scale w_* (Kaimal and Finnigan, 1994).

For an observer near the ground convective cells pass overhead at a speed set by the mean wind velocity in the bulk of the convective boundary layer, U_m, so

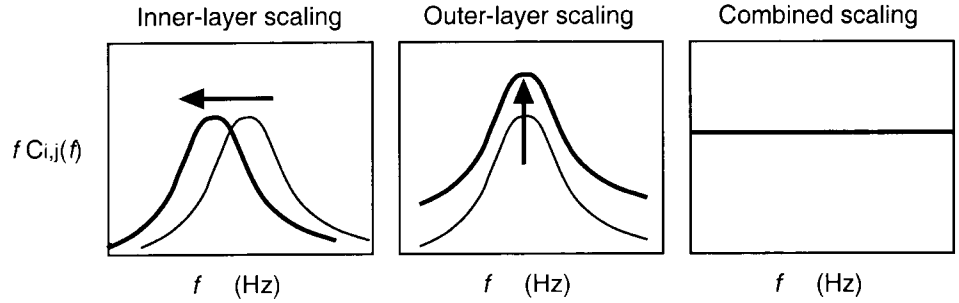

Figure 2. Schematic spectra of fluctuating quantities with arrows showing the effect of an increase in observation height, z, (a) (left-hand side) a spectrum with amplitude insensitive to observation height, as predicted by inner layer scaling (ILS); (b) (centre) a spectrum with position on the frequency axis insensitive toheight, as predicted by outer-layer scaling (OLS); (c) a spectrum with both amplitude and position on the frequency axis insensitive to height, as predicted for combined scaling (CS).

the Eulerian time scale is z_i/U_m. For the same observer we expect the strength of horizontal wind motions to depend on his observation height above ground, which we express as z/z_i. Thus, the normalized spectra depend on a number of parameters, the principle ones given by

$$fC_{i,j}(f) = \chi_*^i \chi_*^j \phi_{i,j}\left(\frac{fz_i}{U_m}, \frac{z}{z_i}\right), \tag{11}$$

where, this time, $\chi_*^1 = \chi_*^2 = \chi_*^3 = w_*$ and $\chi_*^4 = F_{s,0}/w_*$ (Kaimal and Finnigan, 1994).

At this point KY91 argue that convective motions are essentially horizontal near the ground with the spatial pattern of convection being imposed from above. This will be reflected in the frequency composition of the spectrum, which should become independent of height. That is, the OLS component of the observed turbulence spectrum becomes

$$z \ll z_i : fC_{i,j}(f) = \chi_*^i \chi_*^j \varphi_{i,j}\left(\frac{fz_i}{U_m}\right) \zeta_{i,j}\left(\frac{z}{z_i}\right). \tag{12}$$

Equation (12) predicts that the amplitude, but not shape, of the OLS spectrum varies with height near the ground, as shown schematically in Figure 2b. It expresses the general nature of outer-layer scaling (OLS) in the lower part of the convective boundary layer.

3.2.3. *Combined Scaling (CS)*

Following KY91, we now assume that there exists a regime where the frequency and height requirements for the OLS and ILS spectra are both obeyed simultaneously. This leads to a particularly simple form for the CS spectrum. Inner-layer scaling requires shape and amplitude, but not position, of the spectrum to be independent of height, while OLS requires its shape and position, but not amplitude

to be independent of height. To meet both requirements the matched spectrum can vary in neither amplitude nor position on the frequency axis as height changes. KY91 deduce that $fC_{i,j}(f)$ must then be constant, as shown in Figure 2c. That is, the spectrum is of the form

$$z \ll z_i : fC_{i,j}(f) = \chi_*^i \chi_*^j G_{i,j}. \tag{13}$$

Here, χ_*^i and χ_*^j are the appropriate scales and the $G_{i,j}$ are constants. Using inner layer scales, KY91 report the following values for these constants: $G_{1,1} \approx 0.95$, $G_{3,3} \approx 0.35$, $G_{4,4} \approx 0.9$, $G_{1,3} \approx -0.2$, $G_{1,4} \approx -0.6$ and $G_{3,4} \approx -0.2$. Equation (13) states that $C_{i,j}(f)$ should observe a -1 power-law relationship with frequency. Results by KY91, Katul and Chu (1998) and Katul et al. (1996, 1998) show that power spectra with segments displaying such -1 power laws are not uncommon in the atmospheric surface layer. KY91 also report u-T and w-T cospectra with this characteristic. Another prediction of (13) is that the amplitude of the spectrum is independent of height, a feature that has not been highlighted in previous studies.

A problem with this derivation of Equation (13) is that, in our application, there is a conflict on whether we should choose inner-layer or outer-layer scales. In a true matching layer the spectra would depend on both sets of scales simultaneously. Such agreement could only occur fortuitously. A deeper problem is that the argument in KY91 does give any reason why we should expect spectral matching at all in our situation, rather than just a transitional part of the spectrum, or perhaps just superimposed, disjoint spectral components. Our derivation of Equation (13) is therefore at least incomplete. Even so, we will use Equations (10), (12) and (13) to guide our analysis of the experimental spectra. In particular, we will look for CS behaviour where $fC_{i,j}(f)$ is independent of height and frequency.

We will use results from the Kansas experiment (Kaimal et al., 1972) to provide a standard model for the ILS spectra. For our results we will use the Kansas spectra corresponding to L = 27 m as this standard. The inclusion of stability here is not strictly consistent with Equation (10), which has no provision for stability. However, the stable results from Kansas were principally from nocturnal conditions when there was no large-scale convection so, in terms of our conceptual model, they must represent ILS spectra. Again this argument is heuristic; we will revisit it also, after examining the experimental results.

4. Results and Discussion

In this section we present spectral results from Warrawidgee. The various spectra are presented in three ways, according to the features being emphasized and the points being made. When comparing our results with those from the Kansas experiment (Kaimal et al., 1972) we plot the spectra times frequency using a linear scale on the vertical axis and normalized frequency, fz/u, on a logarithmic scale

on the abscissa, consistent with ILS. In these plots the same area under the curve represents the same contribution to total variance or covariance, whatever the frequency, so they make clear the relative importance of various parts of the spectrum. The amplitudes were normalized before averaging, using the ILS parameters u_* and s_* calculated at 2.0 m, and indicated on the vertical axes of these plots. In preparing these plots, the individual spectra were averaged at matching normalized frequencies. In a second class of plots we use natural frequency on the abscissa, and spectra were averaged at matching natural frequency to better present results we expect to obey OLS. We could not scale these correctly on outer-layer parameters because we did not measure the height of the convective boundary layer nor the mean wind speed within it. In a third class of plots we use a logarithmic scale for the ordinate to emphasize power-law relationships displayed by the spectra.

The Kansas spectra we use for comparison in these plots corresponds to $L = 27$ m, which was the harmonic mean Obukhov length observed over all 31 runs. The Kansas spectra define ILS turbulence particularly well in the undisturbed nighttime conditions at Kansas, when larger-scale motions were suppressed and only locally-generated turbulence was present. It is not a foregone conclusion that these spectra are the correct standards for disturbed conditions.

We will often compare our results with those from three other experiments where spectral measurements of wind, temperature and, in two cases, humidity were made in a well-developed surface layer and where the horizontal wind varied substantially at low frequencies. The first of these experiments was conducted by Zermeño-González and Hipps (1997), henceforth ZH97, at two sites in the Cache Valley in UT, USA. Measurements at both sites were made within an advective inversion formed over an irrigated alfalfa field, downwind of dry terrain. We will refer only to measurements from the instruments with the greatest fetches, located at about 300 m from the windward boundary of the fields and at a height of 1.5 m above the 0.35-m high crops. Only the vertical component of wind speed was measured in these experiments, so we infer the variability of the horizontal wind from the general experimental situation and the similarity of the spectral results to those at Warrawidgee. This experiment chiefly serves to show that results like our own are not uncommon near the base of advective inversions.

The other two experiments were conducted in very different situations. One, by Andreas (1987), henceforth A87, was conducted over a level snow field at Grayling, MI, USA, with fetches of 300 m and 150 m to the south and west, respectively, to the toe of forested hills that rose about 80 m within a kilometre of the measurement site; similar forested hills also lay on the other side of the flat valley, at about 6 km to the north. The turbulence instruments were mounted at 2 m. Conditions during this experiment divide almost equally between stable and unstable cases. The other experiment was conducted by Smeets et al. (1998), henceforth SDV98, in a stable surface layer at the base of a katabatic flow on the Pasterze glacier in the Austrian Alps. The glacier was about 1 km wide and 4 km long. Measurements were made at 4 m and 10 m above the melting ice. Data were

selected for cases where the height of the wind maximum in the katabatic flow was greater than 13 m. This also selected for disturbed conditions where forcing by the large-scale wind was significant compared to the katabatic forcing. Humidity fluctuations were not measured in this experiment. We will refer only to the lower measurements, at 4 m over the ice, where flow conditions were expected to be more like those in a classical surface layer.

We will note striking similarities between our experimental results and those of ZH97, SDV98 and A87. This, along with our initial intention to study unsteadiness, leads us to interpret our results in the context of disturbed surface layers, even though previous measurements in situations like ours have used steady 'advection' as the explanatory paradigm (e.g., Lang et al., 1983; ZH97).

A final introductory point concerns the terminology OLS, ILS and CS as we shall use them henceforth. We deal with the spectra of velocity and scalars at levels close to the ground, where large-scale motions are predominantly horizontal so true OLS turbulence cannot exist. Nevertheless, we will use the term OLS to describe spectra near the ground that exhibit the same power distribution as the true OLS spectrum and that vary with height, according to Equation (12). Such motions are presumably driven by the OLS motions above and they will be governed by the same external parameters as the OLS motions above. We will also use the term OLS to describe parts of scalar spectra and cospectra that directly result from these OLS motions and so exhibit a similar frequency spectrum and height dependence. ILS turbulence, on the other hand, is quite familiar. For neutral and stable nocturnal conditions, when OLS motions were suppressed, its spectrum was well defined by the Kansas experiment (Kaimal et al., 1972). For unstable conditions the Kansas results do not discriminate between ILS and other spectral components, so the ILS spectrum alone is not known in unstable conditions. We use the term CS to describe parts of the spectra that are independent of height and frequency, in accord with Equation (13).

4.1. VELOCITY POWER SPECTRA AND COSPECTRA

Shear stress was very nearly constant with height in the surface layer at Warrawidgee. For the 31 runs discussed here u_* increased by 6% on average between 2.0 m and 3.9 m, slightly more than the 2% reported by Laubach et al. (2000) for the same runs plus others with higher wind speed or smaller net radiation. There were substantial shifts in wind strength and direction during most of our 31 runs of 20 min duration. The shapes of the wind power spectra were therefore significantly different to those obtained in steadier conditions (e.g., Kaimal et al., 1972). In this section we present our experimental results and interpret them along lines suggested by Peltier et al. (1996).

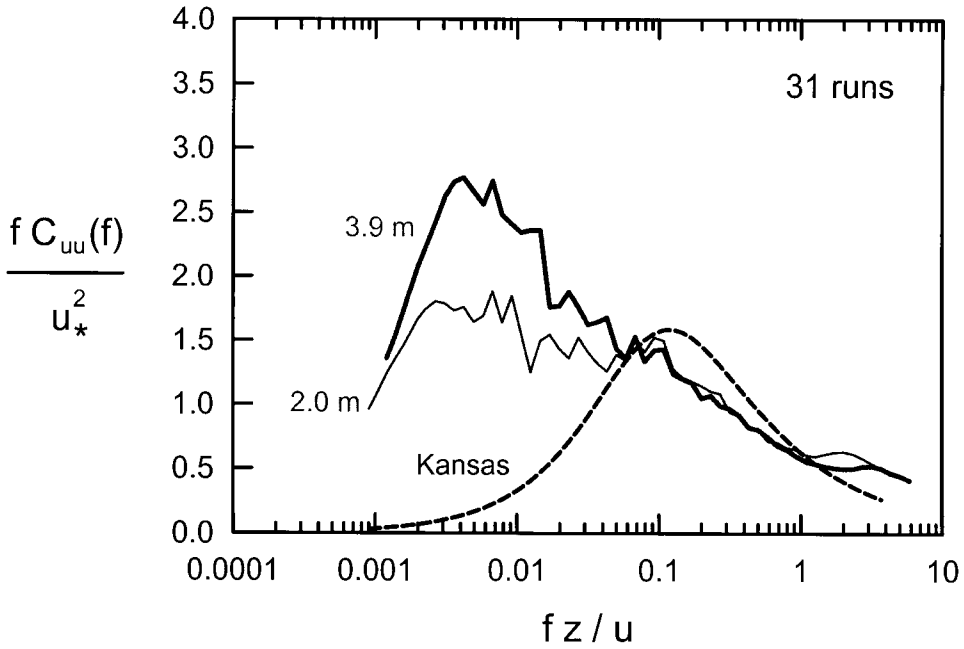

Figure 3. Power spectra of the streamwise wind velocity at Warrawidgee at 3.9 m (thick line), 2.0 m (thin line), and from the Kansas power spectrum (dashed line) for L = 27 m and u_* = 0.37 m s^{-1}, which values were the averages of the 31 runs.

4.1.1. *The Power Spectra of Horizontal and Vertical Wind Velocity*

Figures 3–5 show the power spectra for the longitudinal, lateral and vertical components of wind velocity at 2.0 m and 3.9 m. The frequency axes have been non-dimensionalized so that spectra will be coincident where they obey ILS. The same spectra are plotted on a logarithmic vertical axis in Figure 6 to emphasize power-law relationships.

Both horizontal spectra show substantial variance at low frequencies, reflecting the disturbance by the overhead convection. This effect is larger at 3.9 m than at 2.0 m. The u spectrum then grades continuously downwards towards higher frequencies while the v spectrum shows a very distinct minimum before rising to another peak, at higher frequencies. The w spectrum has no prominent peak at low frequency, in keeping with the general notion that large-scale motions must be essentially horizontal near the ground.

The v Spectra

The prominent minimum in our v spectra is highly unusual. We know of no other v spectrum from the surface layer that displays this feature quite so prominently. Unfortunately, v spectra have not reported by others who have worked in strongly disturbed conditions. Even so, this gap is very fortunate for our analysis because it strongly suggests that our v spectra are composed of two parts, one associated

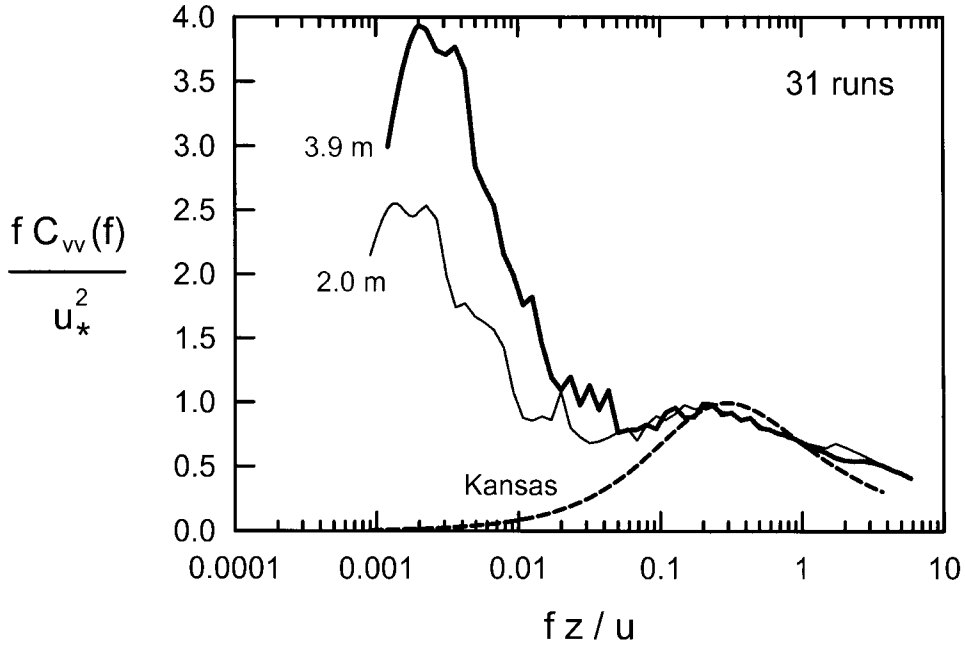

Figure 4. Power spectra of lateral wind velocity. Details as for Figure 3.

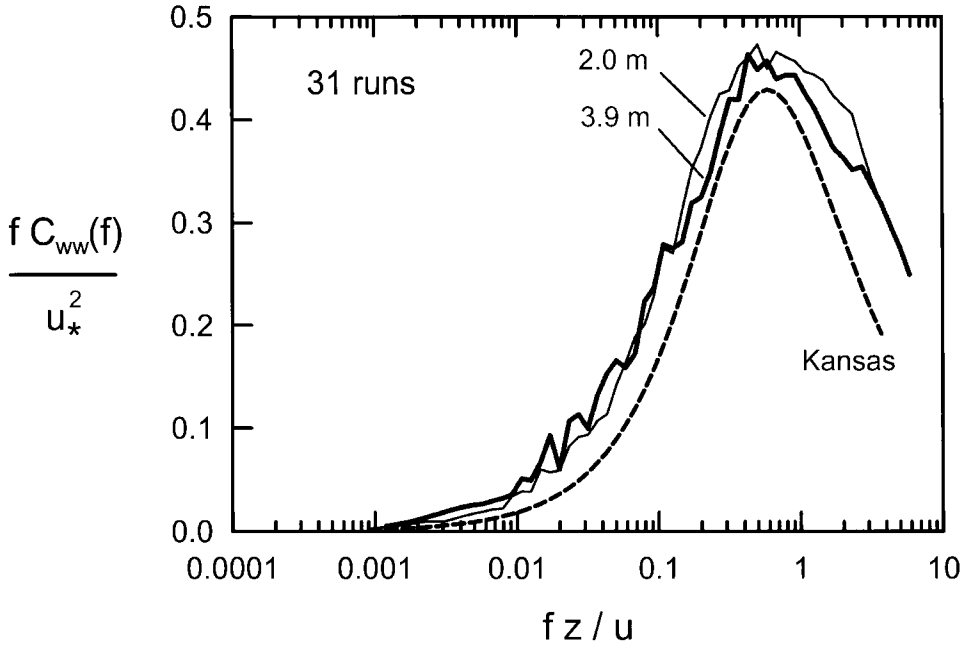

Figure 5. Power spectra of vertical wind velocity. Details as for Figure 3.

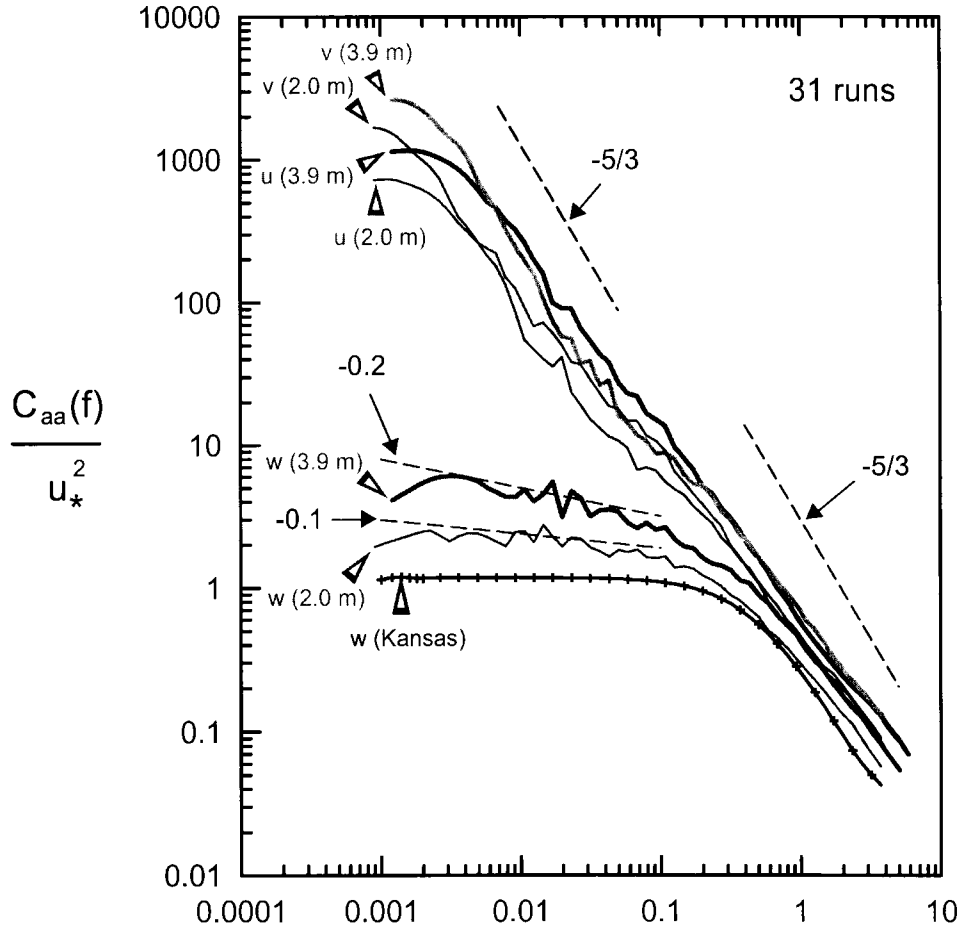

Figure 6. Normalized power spectra for vertical and longitudinal wind fluctuations from Figures 3–5, plotted on logarithmic axes to emphasize power-law relationships.

with the disturbance and the other with shear processes near the ground. This is not a new idea. Indeed Peltier et al. (1996) have developed a spectral model for the surface layer in convective conditions based on just such a division of the spectrum. The novelty of our situation is that we have convective disturbance of a stable surface layer, for which the Kansas results define the ILS spectrum rather well.

Figure 4 shows that the high frequency parts of the v spectra from 2.0 m and 3.9 m are coincident. This means that these spectra obey ILS at these frequencies. As such, we might expect this part of the spectrum to have the same shape as the corresponding Kansas spectrum, which we show superimposed. The observed spectrum has somewhat more power overall than the Kansas spectrum, its peak frequency is lower by about a factor of two and the spectrum is broader. Also the Warrawidgee spectrum falls away as a -1.3 power law at high frequency, rather

than obeying the $-5/3$ power law expected in the inertial sub-range of frequencies (Figure 6).

These differences can be explained in terms of the unsteadiness of the wind during our experiment. The v direction is perpendicular to the mean wind calculated over whole runs. Within runs the wind direction varied, so our v spectra are composites of both the u and v spectra that could have been defined during subintervals of the whole runs. That is, our v spectrum is something of a hybrid of normal u and v spectra: it has a peak frequency and power intermediate between the Kansas u and v spectra. Variations in peak frequency could also explain the observed broadening of the spectrum, as well as distortion of the $-5/3$ region.

The low-frequency parts of the v spectra from the two levels are not coincident on this plot (Figure 4) so they do not obey ILS. Rather, the two spectral peaks occur at the same natural frequency, consistent with OLS. The spectrum at the higher level has considerably more power than at the lower one, the ratio at the spectral peaks being 1.6 : 1. Peltier et al. (1996) propose that at the largest spectral scale the varying horizontal wind field should have the height dependence of the mean wind profile. Indeed, the peak ratio of our v spectra agrees well with the squared ratio of the observed mean wind speeds over all runs at the two levels, $(4.29/3.35)^2 = 1.64$.

The peak frequency corresponds to an eddy size of the order of 1 km, and the spectrum at 3.9 m falls off from the peak towards higher frequencies very nearly as a $-5/3$ power law in the decade $0.003 < fz/u < 0.03$ (Figure 6). This spectrum is reminiscent of the wind spectra typically observed in mixed layers of convective boundary layers (e.g., Kaimal and Finnigan, 1994). This is also consistent with assumptions in the model of Peltier et al. (1996).

At 2.0 m the v spectrum falls off as a -1.4 power law over the range $0.003 < fz/u < 0.03$. This significant departure from the $-5/3$ law is most likely a result of overlap of ILS and OLS parts of the spectrum at frequencies less than 0.05 Hz. The OLS part of the spectrum at 2.0 m is less powerful than at 3.9 m, and therefore less dominant in determining the shape of the combined spectrum. Analysis of Figure 4 shows that the v spectrum at 2.0 m can be constructed from OLS and ILS parts, calculating the OLS component as that at 3.9 m divided by 1.6, and the ILS component as the observed curve at either level extrapolated to lower frequencies. This procedure is plausible rather than rigorous because of uncertainty in how exactly this extrapolation should be done.

A final and intriguing observation on the v spectrum is that, while the ILS part appears to extend to frequencies lower than the gap frequency, the OLS spectra appear to cut off at about 0.05 Hz. At higher frequencies the whole spectrum obeys ILS.

The u Spectra

It is not immediately obvious that the u spectra can also be decomposed into ILS and OLS parts because separate OLS and ILS peaks are not apparent here. Even

so, there are indications that the structure of the u spectrum is similar to that of the v spectrum.

At the highest frequencies the u spectra at the two levels are coincident, indicating that they obey ILS. The u spectrum from Kansas has rather more power than the corresponding v spectrum, and its peak is at lower frequency, so we expect the ILS peak to merge more with the OLS part of the spectrum, tending to eliminate the minimum that separated ILS and OLS peaks in the v spectrum.

At the lowest frequencies the curves obey OLS, as indicated by their peaks occurring at the same true frequency. The ratio of the peak heights is 1.5, not far from the 1.6 observed for the v spectra and with the ratio possibly influenced by greater overlap with the ILS part of the u spectrum. On a double logarithmic plot the u spectra display almost linear segments with slopes of about -1.2 at 2.0 m and -1.33 at 3.9 m in the frequency range $0.03 < fz/u < 0.1$ (Figure 6). These lie between the slope of $-5/3$ characteristic of turbulence in the mixed layer above, and the -1 value for CS turbulence predicted by Equation (13). Our interpretation is that these slopes are simply the result of overlap of independent ILS and OLS parts of the spectrum. This interpretation is not inconsistent with several well-documented observations of wind spectra obeying the -1 power law (e.g., Phelps and Pond, 1971; Katul et al., 1998), but we consider that such results are special cases from a wider range of possible results and have no general validity.

It is not surprising that, in general, the u and v spectra do not obey the -1 power law predicted by Equation (13) for CS turbulence, since these spectra can be described in terms of ILS and OLS components only.

The w Spectra

The w spectra from Warrawidgee are shown in Figure 5. At first sight these are very much like the Kansas spectrum. The curves from the two levels are almost coincident, in keeping with the dictates of ILS. Also, both peak frequency and total power are about the same as in the Kansas spectrum, these being insensitive to changes in wind direction. The main difference with the Kansas spectrum that is apparent in Figure 5 is a noticeable broadening.

We propose that spectral broadening is caused by variability in wind speed. To test this we assumed that the data collected during each run are sampled not from a single spectrum, but from a set of different spectra, each characterizing a different turbulent flow with its own characteristic parameters, u_* and L. We simulated such a situation by constructing a set of Kansas power spectra with a range of parameter values, then formed a composite spectrum as a weighted average of these. We based our simulations on data from three runs on February 5 when spectral broadening was quite evident. We first created a frequency histogram of wind speed, with ranges 0.5 m s^{-1} wide. For each of these ranges we calculated a value of L using a regression relationship between u and z/L obtained from whole runs. Kansas power spectra were then calculated for each range and averaged, weighing the individual spectra according to frequency of occurrence. The results were broadened power

spectra that looked much like the experimental ones. That is, the broadening displayed by the w power spectrum in Figure 5 is consistent with the Kansas spectrum in its main features if allowance is made for the unsteady conditions experienced during the individual runs.

The other difference between our spectra and the Kansas spectrum only becomes apparent when the w spectra are plotted on a logarithmic ordinate as in Figure 6. This shows that the w spectra from Warrawidgee are not coincident for $fz/u < 0.2$, but obey -0.1 and -0.2 power laws at 2.0 m and 3.9 m respectively. This is significantly different to the 0 power law of the standard spectrum derived from the Kansas experiment, even allowing for spectral broadening. Others who have worked in disturbed conditions (SDV98; A97) have also reported enhanced variability of the vertical wind at low frequencies. Such enhancement is not restricted to notably unsteady conditions. It has also been noticed by Högström (1990) in data taken over agricultural land in a situation that was much less obviously disturbed. Högström had previously screened his data to remove non-stationary runs. (Högström's result is interesting in that he attributes the additional variance to 'inactive turbulence', and provides a great deal of information on turbulence at the site to support this.) In our case we label the additional turbulence as OLS, using its height dependence as the distinguishing feature, in accord with Equation (12).

Enhancement of the w spectrum at low frequency is also a feature of the model of Peltier et al. (1996). Their explanation, in simple terms, is that variations in velocity of the predominantly horizontal motions near the ground necessarily involve areas of convergence and divergence in the horizontal wind, so continuity demands there be transfer of spectral energy from the horizontal to the vertical air motions. Thus the w spectrum is enhanced at low frequency as a direct consequence of the OLS motions and the enhancement bears the shape of the OLS spectrum. The total amount of energy involved is rather small, so this transfer has an imperceptible effect on the observed u and v spectra.

It appears likely that these w motions are associated with coherent downdrafts and updrafts. These have often been observed in convective conditions over uniform ground. Powerful downdrafts were also observed by SDV98 in conditions highly disturbed by topographically-induced turbulence. Such vertical fluctuations, originating in the horizontal motions, must also transport momentum and so transfer energy back into horizontal variance. This would produce highly coherent motions that are very effective in modulating momentum transport to the ground (e.g., Haugen et al., 1971; Wilczak, 1984). High *u*-*w* coherence at low frequencies has been noted by A87 where the OLS motions were topographically induced.

The above comments do not imply that spectral kinetic energy flows exclusively from the horizontal motions into the updrafts and downdrafts. The source of the kinetic energy is the convective motions on the larger scale, so the vertical motions might better be viewed as the agent that transfers momentum from the large-scale, three-dimensional turbulence down towards the surface to drive the fluctuations in

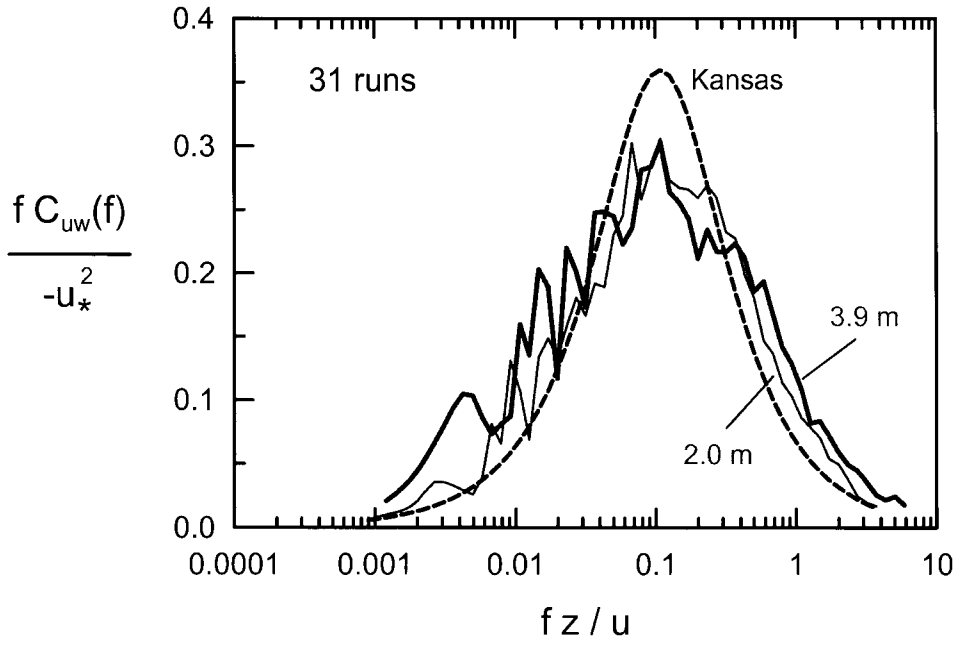

Figure 7. The normalized u-w cospectrum at 2.0 m (thin line) and 3.9 m (thick line) compared to the Kansas cospectrum for L = 27 m.

the horizontal wind profiles near the ground. This view correctly predicts stress gradients within updrafts, as observed by Haugen et al. (1971) in a burst at the Kansas site.

4.1.2. *The Momentum Cospectra*

Figure 7 shows the average of the normalized u-w cospectra, $-fC_{uw}(f)/u_*^2$. Also plotted is the Kansas u-w cospectrum (Kaimal et al., 1972) calculated for L = 27 m. The observed spectra have peaks at about the same normalized frequency as the Kansas spectrum, but the experimental cospectra again are somewhat flatter and broader. Again we propose that this broadening is caused by the general unsteadiness of wind speed and direction during the runs. There are also significant irregularities for $fz/u < 0.03$. These reflect the much larger irregularities observed in the individual runs, indicating erratic events that transferred considerable momentum; averaging over 31 runs has smoothed these out, but not completely. The irregularities at the two levels match at the same natural frequencies rather than normalized frequencies, consistent with low frequencies representing large-scale motions that affect both levels simultaneously. The broadening and irregularities aside, our averaged momentum spectra are consistent with the Kansas spectra for the two levels.

Similar irregularities in the momentum spectrum at low frequencies have been observed by A87 and SDV98. A87 noted that the irregular peaks of the individual

momentum spectra were frequently negative while the averaged momentum spectrum was similar to the Kansas spectrum. A87 also noted variable, but often large, coherence between u and w at low frequencies, indicating that motions at this scale were well organized, if erratic in their occurrence. SDV98 made similar observations.

Our interpretation of these results follows on from our discussion of coherent structures in the form of updrafts and downdrafts, above. We argue that momentum transfer towards the ground is itself irregular both in strength and direction when the surface layer is disturbed by irregular motions on the larger scale. Momentum transfer can then be viewed as the sum of a steady component, associated with the mean wind, and a random component associated with the disturbance. The steady component gives rise to a momentum spectrum of the standard shape. The irregular component gives rise to erratic contributions in random directions. These disturbances therefore produce variability in the momentum flux, but their contribution to the vector total momentum flux is zero. The u and w power spectra over the paddy at Warrawidgee (Figures 3 and 4), the snow field at Grayling (A87) and the Pasterze glacier (SDV98) are all consistent with this explanation.

4.2. SCALAR POWER SPECTRA AND COSPECTRA

We now present the scalar spectra and cospectra from Warrawidgee, basing our interpretation on the above analysis of the velocity spectra.

4.2.1. *Power Spectra of Scalars*

Figure 8 shows the power spectra of the set of scalars at 2.0 m and 3.9 m, averaged over the 31 runs and plotted on a logarithmic axis to highlight power-law relationships. The spectra of all scalars are almost coincident at each level, except at the highest and lowest frequencies.

At the highest frequencies, $fz/u > 0.1$, the c and q curves from the two levels are almost coincident and they fall off approximately as the $-5/3$ power law. The temperature spectra and the α and d spectra, which are calculated using T measurements, have less negative slopes, especially at the lower level. We attribute this to noise in our temperature data. Discounting this, all spectra obey ILS very well at high frequencies.

At intermediate frequencies, between $0.007 < f$ and $fz/u < 0.1$, all scalar spectra coincide and observe the -1 power law very well, so they conform to the CS relationship (13) in this range.

At the lowest frequencies, for $f < 0.007$, the various power spectra are not coincident. Instead the variances decrease in the order c, α, q, d at 2.0 m. Scalars c, α and d are therefore in the order predicted from theory. Humidity, q, lies between α and d while the behaviour of temperature is rather more complex, its position depending on frequency. Perhaps temperature behaves like this because heat storage in the water and vegetation depends on temperature in a frequency-

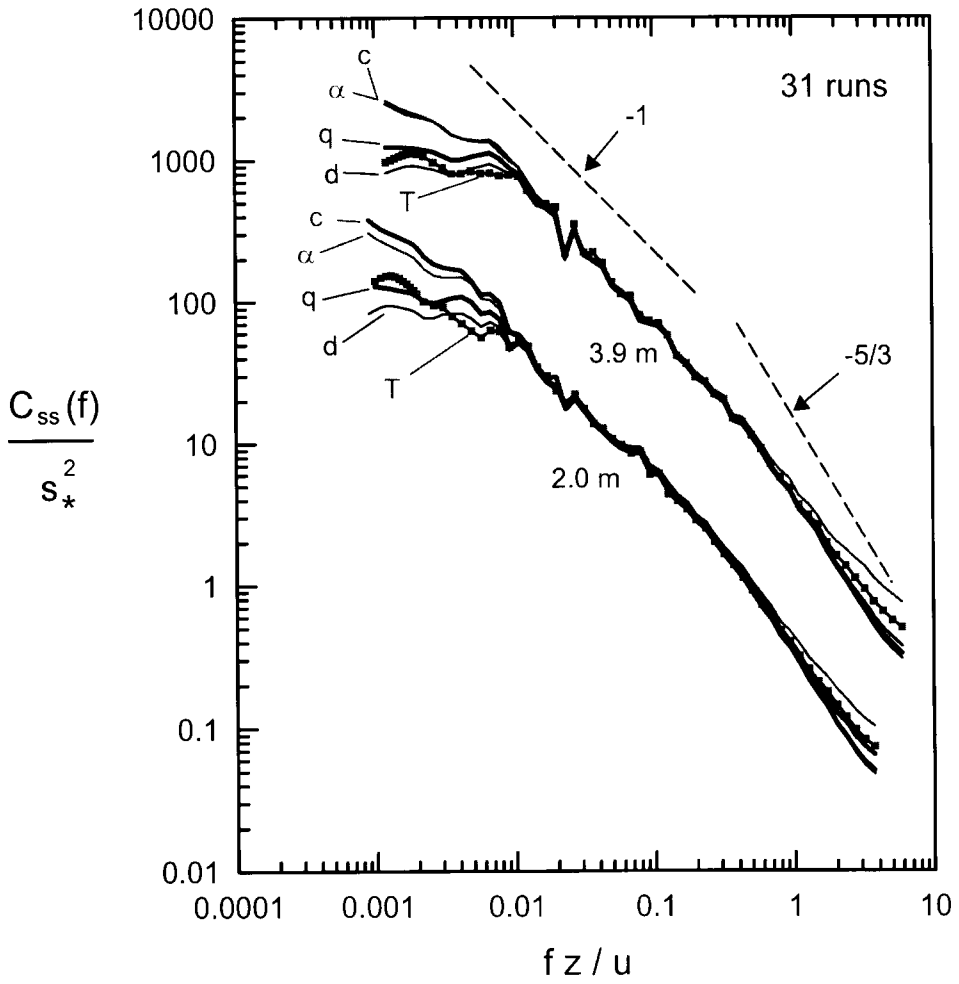

Figure 8. Normalized power spectra of carbon dioxide concentration, c, equivalent temperature, α, specific humidity, q, saturation deficit, d, and temperature, T, at 2.0 m and 3.9 m. The spectra at 3.9 m have been shifted a decade to higher amplitudes.

dependent way. Alternatively, or in addition, this behaviour may reflect an OLS component of temperature variance, originating upwind and advected over the site. The second mechanism may explain the change in ordering at 3.9 m, where the α. spectrum has increased to become almost coincident with the c spectrum. The α curve is calculated using the T data, so advected variance would enhance the α spectrum, especially at the upper level.

Enhanced scalar variance with differences between scalar species have been noted before in disturbed conditions. A87, working over snow, found the variability of temperature to be slightly more enhanced than that of humidity at the lowest frequencies. Over irrigated alfalfa ZH97 found that the variance of humidity was

more enhanced than that of temperature, which behaved very much like saturation deficit. SDV98 observed only temperature fluctuations but noted large variance at low frequency. A87 explained his results in terms of an advected scalar field, through our results suggest that this explanation is not correct for our q and c spectra. We observed enhanced c and q variance at low frequencies in the absence of significant OLS fluctuations in those variables. For T, any effect of advected temperature variance was small at our site, even though the conditions for it were much more favourable than over the snow field studied by A87. On the other hand, SDV98 and ZH97 appeal to the action of large eddies bringing in air from above the local boundary layer to explain their results. This argument is also unsatisfactory, as shown below.

4.2.2. *Power Spectra of Surface, Mid-Canopy and Air Temperatures*

Figure 9 shows the temperature spectra at the two levels together with the spectrum of surface temperature, T_s, measured remotely with the infrared thermometer, and of air temperature within the rice canopy, measured at about 2/3 crop height above water level. Slow time response of the Vaisala sensor within the canopy and noise spikes in the raw signals make the power spectrum of canopy air temperature unreliable at frequencies greater than 0.02 Hz. Natural frequency is used on the ordinate here because normalized frequency is inappropriate within the canopy.

The two main features of the spectrum of surface radiometric temperature are that its maximum is at very low frequency and that it falls off as the $-5/3$ power law at higher frequencies. These same features are prominent in the spectra of surface temperature reported by Lagouarde et al. (1997) for the Landes forest canopy, using observations at 40-m resolution made from a hovering helicopter, and by Katul et al. (1998) for the surface temperature of grass growing in a large clearing at Duke Forest.

The remarkable similarity of these spectra across a wide range of surfaces and conditions suggests that they reflect conditions in the convective boundary layer above each site rather than at the surfaces themselves. Indeed, the shapes of these surface temperature spectra are very like typical wind spectra observed at mid levels within convective boundary layers (e.g., Kaimal and Finnigan, 1994). Our T_s spectrum also has much the same shape as the OLS part of the v spectrum observed at 3.9 m at Warrawidgee (Figure 6). That is, the shape of the spectrum of radiometric surface temperature appears to reflect directly the shape of the 'disturbing' wind fluctuations overhead. As such it obeys OLS.

Comparison of this surface temperature spectrum with that within the canopy air space and those in the air above reveals other interesting features. At the lowest frequencies, variance at the surface exceeds variance within the canopy, and both of these exceed the variance in the air above. This is evidence that the surface temperature fluctuations originate at the ground.

To understand how this might be so, consider ground that emits a constant flux of scalar. Suppose further that the effective eddy diffusivity of the atmosphere

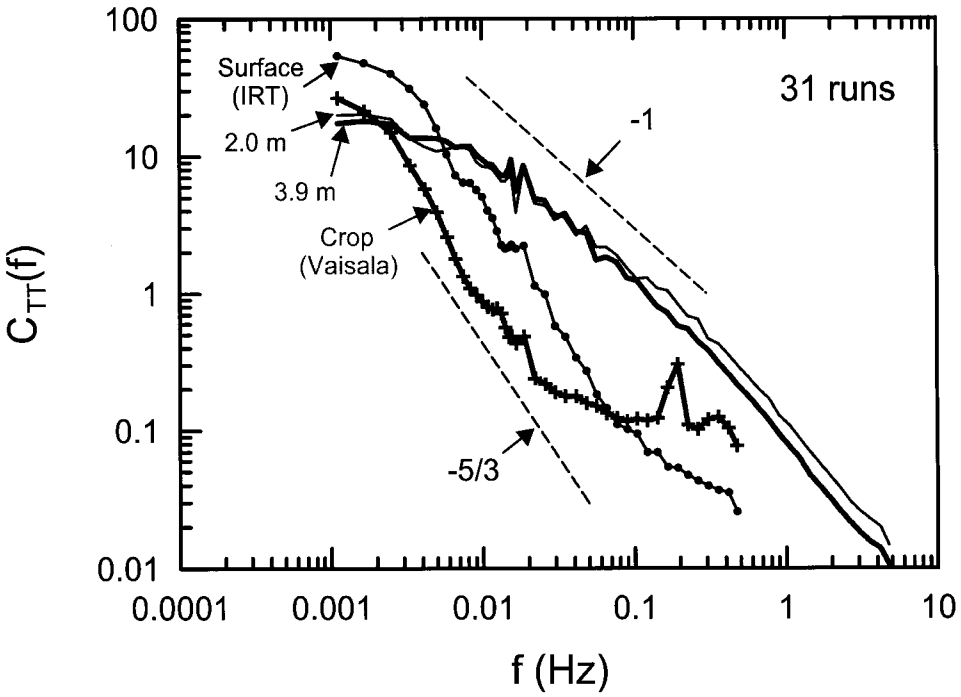

Figure 9. Power spectra of surface temperature measured with an infrared thermometer, air temperature within the crop at 2/3 crop height, and air temperature at 2.0 m and 3.9 m.

above varies in proportion to the OLS component of the horizontal wind spectrum, as would be the case if 'fast' ILS turbulent velocity fluctuations maintained continuous equilibrium with the 'slow' OLS stress changes. Scalar concentration would then tend to build up near the ground when wind speed is low, and to dissipate when wind speed is high. That is, a concentration increase would follow a wind speed decrease, but with a phase lag. This explanation is supported by Figure 10, which shows a section of data where the standard deviation of vertical velocity, σ_w, calculated from 30-s segments of the w time series, is compared with 30-s averages of u and T_s. The σ_w variations are positively correlated and in phase with the filtered horizontal wind speed, but negatively correlated and lead those of filtered T_s. We expect σ_w to be proportional to the eddy diffusivity near the ground. The relationship with u was not always quite so clear as in this snippet of data, but in our 31 runs the correlation coefficients between the 30-s values of σ_w and T_s were typically in the range -0.6 to -0.8. If surface concentration were held constant, rather than the surface flux, then the scalar flux would vary inversely with wind speed but there would be no contribution to the concentration variance spectrum. For temperature at Warrawidgee, changing wind speed did cause the flux to vary, and the effect of this was to reduce surface temperature variance at low

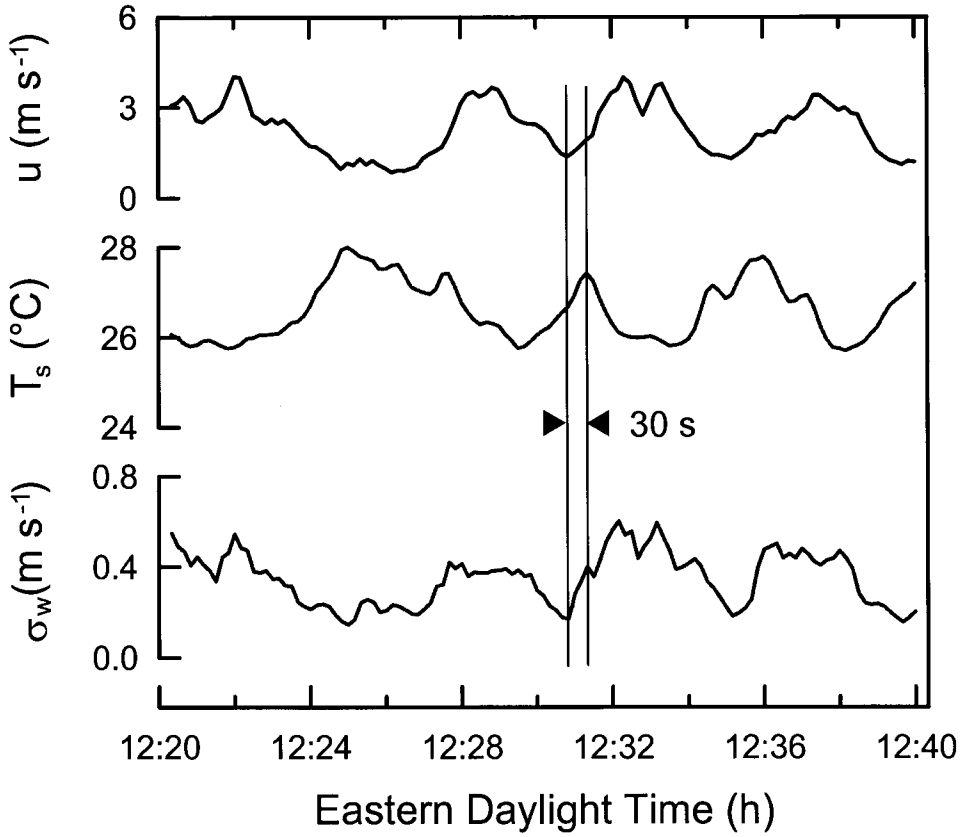

Figure 10. Low-pass filtered time series of streamwise wind velocity at 2.0 m, u, surface temperature measured by an infrared radiometer, T_s, and standard deviation of vertical velocity, σ_w. The plotted values were calculated as the averages and the standard deviation from 30-s segments of the original time series. The data window was advanced in 10-s steps. The vertical lines shown indicate matching valleys on the u and σ_w curves, and the delayed peak in T_s. Data were recorded on 5 February, 1997 at Warrawidgee.

frequencies. This, however, does not seem to have obscured the basic dependence of surface temperature on the OLS component of wind speed.

The temperature spectrum observed within the air space of the rice canopy behaves rather like that of T_s, though variance is generally smaller, as shown in Figure 9. A '$-5/3$' part of this spectrum is also apparent. At frequencies greater than 0.02 Hz this spectrum is influenced by electrical noise. The low-frequency peak and the $-5/3$ spectral region in the range $0.003 < f < 0.01$ are not evident in the air well above the crop. Instead the spectra there are nearly equal at 2.0 m and 3.9 m and they follow a -1 power law; this behaviour is in agreement with Equation (13) for the CS regime.

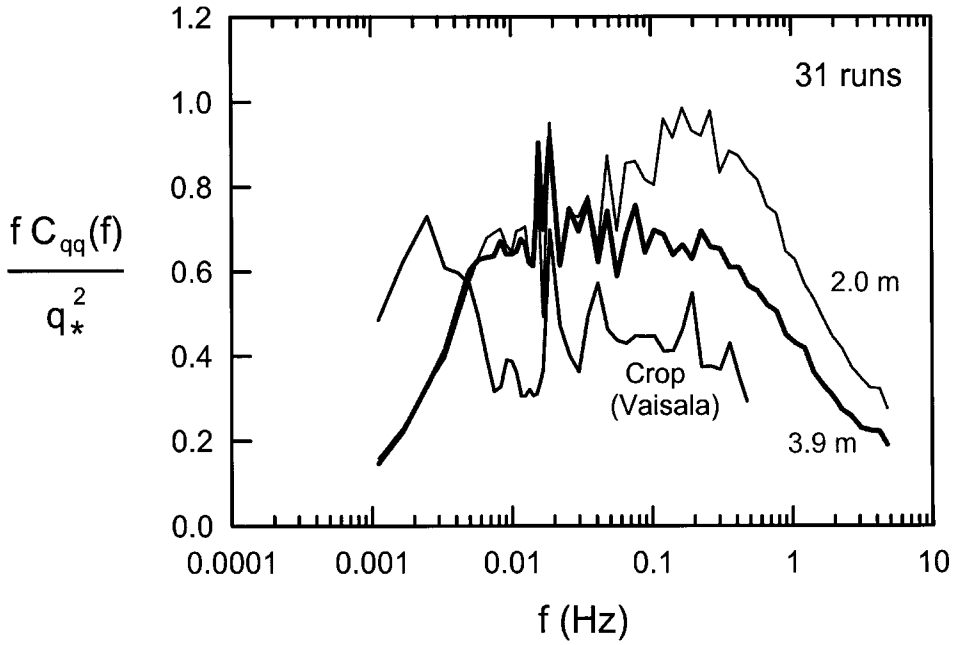

Figure 11. Power spectra for specific humidity within the rice canopy and at 2.0 m and 3.9 m above the displacement height of the crop. All three spectra are scaled using q_* at 2.0 m.

4.2.3. *Changes in Humidity Power Spectra with Height*

Here we plot our results as normalized fC_{qq} on a linear axis to emphasize behaviour in the ILS and CS parts of the spectrum. Figure 11 shows the power spectra of air humidity at about 2/3 crop height above water level, and at 2.0 m and 3.9 m above the displacement height. Specific humidity within the crop was calculated by combining data from the temperature and relative humidity transducers of the Vaisala probe. Again, electrical noise affected our Vaisala data and so the humidity spectrum at frequencies above about 0.02 Hz is not reliable.

The pronounced spectral peak displayed by the mid-canopy humidity at 0.003 Hz is not visible in the power spectra at 2.0 and 3.9 m. Instead they rise together to a shoulder at about 0.007 Hz and are then nearly coincident and constant for about a decade. This horizontal section conforms to the prediction of (13), consistent with CS. We find $G_{4,4}$ = 0.6, rather smaller than the value of 0.9 reported by KY91. It seems that the CS part of the spectrum dominates the OLS part at these frequencies, so the total variance observes CS.

The height invariance of the CS part of the humidity spectra, apparent between the 2.0 m and 3.9 m levels in Figure 10, does not extend down to the ground as shown by the reduced variance within the crop at these frequencies. Indeed, the CS component of the spectrum must vanish altogether between 2.0 m and the surface itself, in agreement with the temperature results, where a true surface spectrum is available. The layer where this happens is the ‘roughness sublayer’ where Equation

(10), and so Equation (13), is not applicable. This means that the CS variations in scalar concentrations do not modulate the surface fluxes, such modulation being associated solely with the OLS part of the spectrum. Variations of scalar concentration at the surface, and the differences in scalar spectra resulting from that, is a clear signature of the OLS parts of those spectra.

At high frequencies we might expect the humidity spectrum at both levels to conform to ILS. Our results confirm this when plotted against fz/u, but only for $fz/u > 0.4$. In the range $0.04 < fz/u < 0.4$ the spectrum at 2.0 m shows a peak, while the spectrum at 3.9 m falls away progressively towards higher frequencies. ILS scaling for a uniform surface layer predicts equal peaks at both levels. This discrepancy suggests we should consider the effects of advection and flux divergence on our results. We will do this in the course of our analysis of the scalar covariance spectra, below.

4.2.4. *Changes with Height in the Cospectra for Scalar Fluxes*

Advection effects were always a possibility at our measurement site. Indeed, an important reason for making measurements at the upper level, at 3.9 m, was so that flux divergence could be observed directly and taken into account in our interpretation. Overall, our measurements show that scalar fluxes differed by about 7% between the two levels (Laubach et al., 2000). We now compare the scalar flux cospectra at the two levels, choosing CO_2 as a representative scalar.

Figure 12 shows the w-c cospectrum at 2.0 m and at 3.9 m, both normalized by the flux at 2.0 m. Also plotted is the Kansas cospectrum, with amplitude adjusted by eye to match the experimental curves for $fz/u > 0.4$. Four features are worthy of note. Firstly, the w-c cospectrum at 2.0 m matches the Kansas cospectrum down to at least the peak of the Kansas spectrum at $fz/u = 0.2$ while, the spectrum at 3.9 m matches only down to $fz/u = 0.4$. Secondly, there was significant flux divergence within the frequency range $0.05 < fz/u < 0.4$. Thirdly, the cospectra at 2.0 m and 3.9 m are similar to each other at frequencies in the range $0.008 < fz/u < 0.05$, and both are consistently larger than the fitted Kansas cospectrum. Finally, at the lowest frequencies, $0.008 < fz/u$, there was a small amount of flux convergence, amounting to a few percent of the total flux. At these lowest frequencies there was a consistent and systematic difference in behaviour between the various scalar species (see Figure 13), indicating that this part of the spectrum obeys OLS.

Confinement of flux convergence to a narrow range of mid frequencies is a new and unexpected result, and one that demands an explanation. We can understand that the spectra are similar at the highest normalized frequencies, $fz/u > 0.4$, because there the transporting eddy motions have heights that are small compared with the distance up to non-equilibrium parts of our scalar profiles. The scalar profiles on our site were probably quite like equilibrium profiles up to at least 3.9 m, as shown by model calculations (Laubach et al., 2000 and unpublished results). Motions on scales much smaller than this are not expected to be affected by the non-equilibrium conditions higher overhead. Therefore, spectra and cospectra at

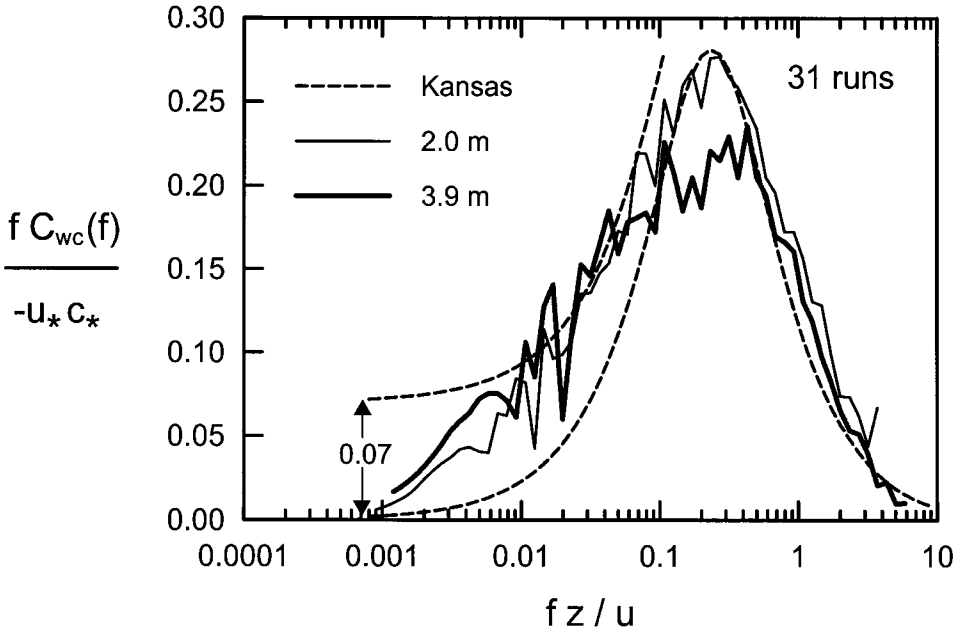

Figure 12. Cospectra of vertical wind and CO_2concentration at 2.0 m and 3.9 m. Both cospectra are normalized using the observed $\overline{w'c'}$ at 2.0 m, so the difference between the curves represents flux divergence. Also shown is the Kansas cospectrum for L = 27 m, reduced in amplitude to fit the cospectrum for $fz/u > 0.4$, and the same cospectrum displaced upwards by 0.07 to indicate the effect of addition of spectrally uniform CS covariance.

high frequencies are the same as those found over homogeneous sites. However, as their sizes increase, eddies begin to carry air down from levels where the scalar profile departs from the equilibrium form. The situation is illustrated schematically in Figure 14. The flux cospectrum then departs from the Kansas model.

To make this observation a little more quantitative we note that the most effective eddies for transporting flux past an observer are centred at observation level and have heights about twice the observation height. The cospectral peak in Figure 12 therefore corresponds to 'most effective' eddies of about 4 m and 8 m eddy heights at 2.0 m and 3.9 m, respectively. Near the peak of the spectrum, the most effective motions therefore move scalars about principally within the equilibrated lowest 4 metres of the profile. At 3.9 m they move them from as high as 8 m where the profile, though not observed, was probably not fully adjusted. At 2.0 m therefore the cospectrum near the spectral peak conforms to the Kansas model, while at 3.9 m the flux is reduced. Flux therefore converges between the two levels. This can safely be attributed to advection.

Extension of the above argument to even larger eddies would predict reduced covariance at all low frequencies, contrary to observation. Figure 12 shows increased flux at both levels compared to the fitted Kansas model, with no divergence

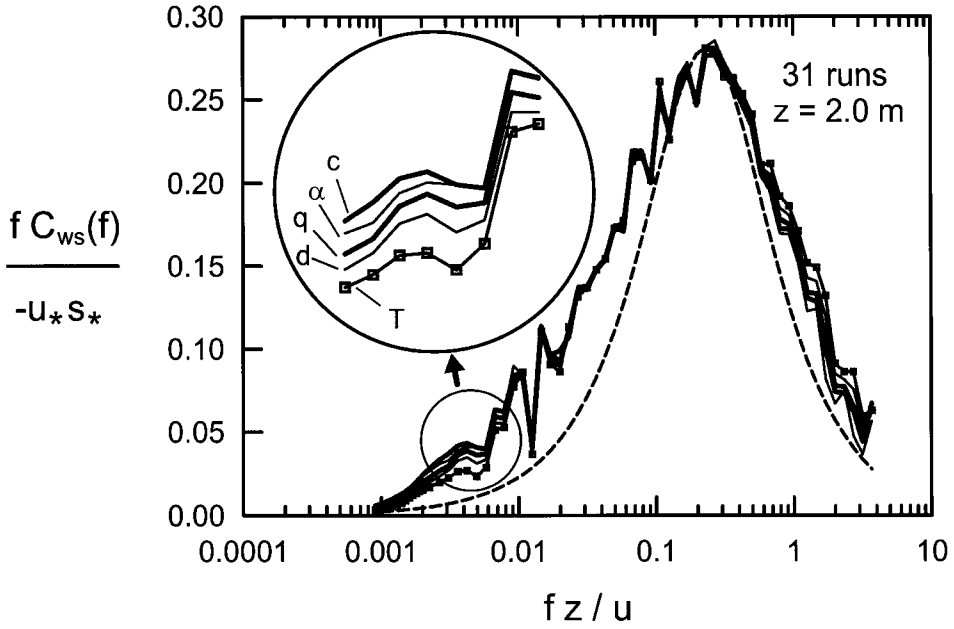

Figure 13. The w-s cospectra at 2.0 m for c, α, q, d and T. These cospectra are essentially identical except at the lowest frequencies, where they rank in order of decreasing sensitivity of flux of each scalar to its surface concentration.

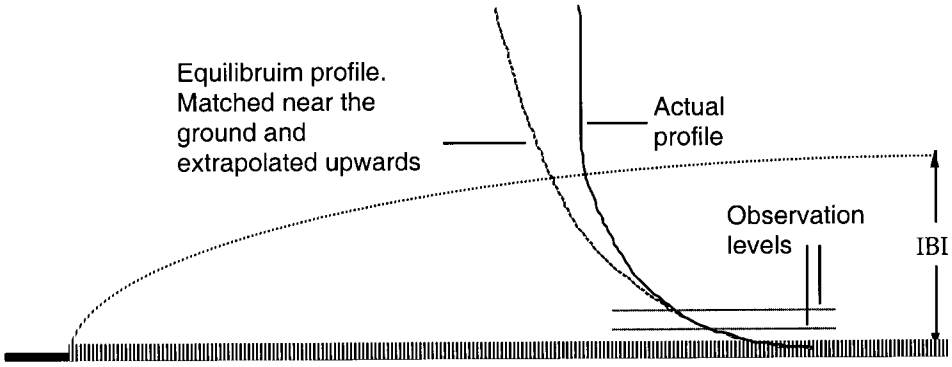

Figure 14. Schematic diagram of scalar profiles in the proposed situation at Warrawidgee. The profile for homogeneous conditions is the standard profile predicted by Monin–Obukhov similarity theory, based on surface values of u_*, s_* and L. Eddies with sizes twice observation height, and centred at the observation height, bring air down from levels where the mean profile is far from the equilibrium one for the upper observation level, but not the lower level.

in the range $0.008 < fz/u < 0.05$. Cospectral enhancement like this has also been observed by others who worked in disturbed conditions (Lang et al., 1983; A87; ZH97; and SDV98). Lang et al. (1983) did not report their horizontal wind spectrum, but their experimental situation was very similar to ours in the same area. SDV98 also reported no temperature flux divergence between 4 and 10 m despite considerable momentum divergence. Both Lang et al. (1983) and SDV98 explained their results in terms of the effect of intermittent large eddies moving air down from near the top of an inversion layer. These explanations fail because, correctly applied, they predict that larger eddies should carry less flux than usual, not more.

In searching for an alternative explanation for these spectra we note that the enhancement of the scalar flux at low frequencies is probably not an 'advection' phenomenon *per se* because the most strongly enhanced spectra were obtained by SDV98 who worked on a glacier with no apparent surface heterogeneity. Nor does its existence seem to depend on the stability of the surface layer, because A87 observed this phenomenon in both stable and unstable conditions. Instead, the common factor seems to be disturbance of the surface layer by a varying wind, caused by overhead convection (present results; Lang et al., 1983; ZH97) or uneven upwind topography (A87; SDV98).

Accordingly, we examine the spectrum to see if it bears the identifying signs of CS turbulence, like the corresponding variance spectrum. Clearly Equation (13) does not describe this region of the spectrum directly since the amplitude of the whole cospectrum increases with frequency. However, we can obtain a good fit of the CS model if we suppose that CS covariance is an additive component of the spectrum, and we fit it by adding a constant amount to the ILS component predicted by the fitted Kansas spectrum. The procedure is indicated in Figure 12, where the Kansas curve has been displaced upwards by 0.07. The CS model fits if the CS covariance is an additive component of the cospectrum described by $fC_{3,4}(f) = 0.07$.

This raises another question of interpretation. Linear addition suggests that the CS component of the covariance spectra derives from localized flux events which fill only a small fraction of space. Fourier spectra combine information both on the form of individual events and on the intervals between them. An increase in the power or number of large, isolated flux events would cause the cospectral density increasingly to represent the intervals between these events, and so to appear at lower frequencies in the Fourier cospectrum. Our results therefore suggest that OLS motions initiate coherent structures which carry much of the flux, or influence their size or spacing. This interpretation is supported by the observation that our individual spectra and cospectra were notably irregular, so that the frequency independence of the CS scalar spectra emerged only after averaging many runs. Irregular spectra and large flux events were also observed by others who have worked in disturbed conditions (A87, ZGH97, SDV98).

At the lowest frequencies, $fz/u < 0.008$, the curves at the two levels diverge a small amount, and their minor peaks match in true frequency (0.0025 Hz). This frequency is the same as that of the OLS peaks of the v spectra (Figure 4) and the within-canopy q spectrum (Figure 11). One should be careful when interpreting fine detail from such a poorly-sampled part of the spectrum as this. However, we believe this peak is real and does represent an OLS component of the flux. Aside from this frequency match, three other considerations support this interpretation. Firstly, the peak increases with height in accord with Equation (12), and since the same large eddy structures were sampled at both levels, this can be taken as significant. Secondly, we see in Figure 13 that the covariances of the various scalars are spread out in the decreasing sequence c, α, q, d and T near this peak, as expected for OLS parts of the spectrum (see also Figure 15, discussed below). The same sequence was also observed at 3.9 m (not shown). This sequence derives from non stochastic relationships that will be expressed within any sample, whether representative or not. Thirdly, we know that all of the flux is carried by OLS in the main part of the CBL. Flux transfer to OLS motions probably occurs progressively over the whole depth of the surface layer, so we expect OLS motions to carry a very small part of the flux even as low as 2 m. This OLS component is of little direct significance in our results, but its identification provides a warning that it may be quite important when measurements are made at greater heights, as from towers over forests.

With the above interpretation of the scalar flux spectrum we now revise the assessment by McNaughton and Laubach (1998) that the measurements at 2.0 m at Warrawidgee were influenced by advection. We based this earlier assessment on the similarity of the shape of our scalar flux spectra to the 'advection' spectra reported by Lang et al. (1983) and ZH97. We now believe that the distinctive shape of the flux spectrum reflects disturbance, not advection. Indeed 'advection' would have caused a cospectral depletion at the low frequencies where we observed enhancement. At 3.9 m some advective effects are noticeable.

In summary, we find that we could find no sign of advective influence in the scalar cospectrum observed at 2.0 m, so we believe it represents an equilibrium spectrum for the disturbed surface layer. This spectrum has large ILS and CS components, and a small but detectable OLS component.

4.2.5. *Cospectra of the Streamwise Scalar Fluxes*

Figure 15 shows the cospectra of the streamwise fluxes for the various scalars at 2.0 m and 3.9 m. Of all of our results, these plots most clearly show the influence of the different lower boundary conditions. The cospectra for c, α and d decrease in the order predicted at low (OLS) frequencies. We note that T behaves normally here, unlike in Figure 8. We note that fluctuations associated with 'advected variance' would be uncorrelated with u' or w' and so would not affect our cospectra. The wide separation of the cospectra for the various scalars here clearly defines the OLS part of the spectrum. This is obvious at frequencies below 0.02 Hz. OLS

covariances are smaller at 3.9 m than at 2.0 m, providing further support for the idea that their origin is at the ground.

At higher frequencies the cospectra at each level are rather similar for all scalars. For $fz/u > 0.1$ the cospectra are also very similar between levels, so the cospectra obey ILS at these high frequencies. The shapes of the cospectra differ significantly between levels at lower requencies. The peak at $fz/u = 0.08$ is significantly larger at 2.0 m than at 3.9 m. This peak is in the frequency rangefound to be influenced by advection in other scalar spectra and cospectra.

There appears to be a horizontal section of the spectrum (-1 power law) at intermediate frequencies at 2.0 m. This conforms to Equation (13) with $G_{1,4} = 0.7$. KY91 give $G_{1,4}= 0.6$, citing their earlier work. At 3.9 m there is a level section at the same height in the neighbourhood of $fz/u = 0.04$, but near $fz/u = 0.01$ the spectrum then reaches a peak. This peak probably arises from greater overlap between CS and OLS parts of the spectrum. The shape of the OLS part seems to be changing with height. For comparison, the $fC_{uT}(f)$ plot of SDV98 is also roughly horizontal for 4.0 m and 10.0 m heights, but with $G_{1,4} = 0.3$ (Paul Smeets, personal communication, 1998). Overall, horizontal flux spectra do seem to display a section that is horizontal and independent of height, in agreement with Equation (13), but $G_{1,4} = 0.6$ does not appear to be a universal value.

5. Scaling Spectral Components

The analysis above shows that all our scalar spectra and cospectra can plausibly be divided into ILS, OLS and CS components. These components are characterized by the way they depend on height and frequency. In this they obey Equations (10), (12) and (13). However, the amplitudes of our spectral components are not consistent with the scales used in KY91. This is not surprising given the very different situation considered by KY91. The common feature appears to be an interaction between features of the surface layer that obey ILS and OLS. Here we suggest the correct scales for our application.

The OLS component of the horizontal motions are associated with an OLS velocity scale, say v_*, which must be the correct velocity scale to be used in Equation (12). This scale can be identified with the convective velocity scale w_* when the disturbance is by convection in the CBL (Panofsky, 1977). We note that at Warrawidgee w_* would depend on parameter values effective over the dry plain rather than local values over the paddy. We have no parameterization for v_* when it characterizes topographically-induced motions. We have argued above that a likely origin of a CS component of spectra and cospectra is by OLS motions, with velocity scale v_*, controlling the occurrence of ILS flux events with velocity scale u_*. The CS components of scalar spectra and cospectra resulting from this interaction would then have the velocity scale $\sqrt{u_* v_*}$, which should then be used in (13).

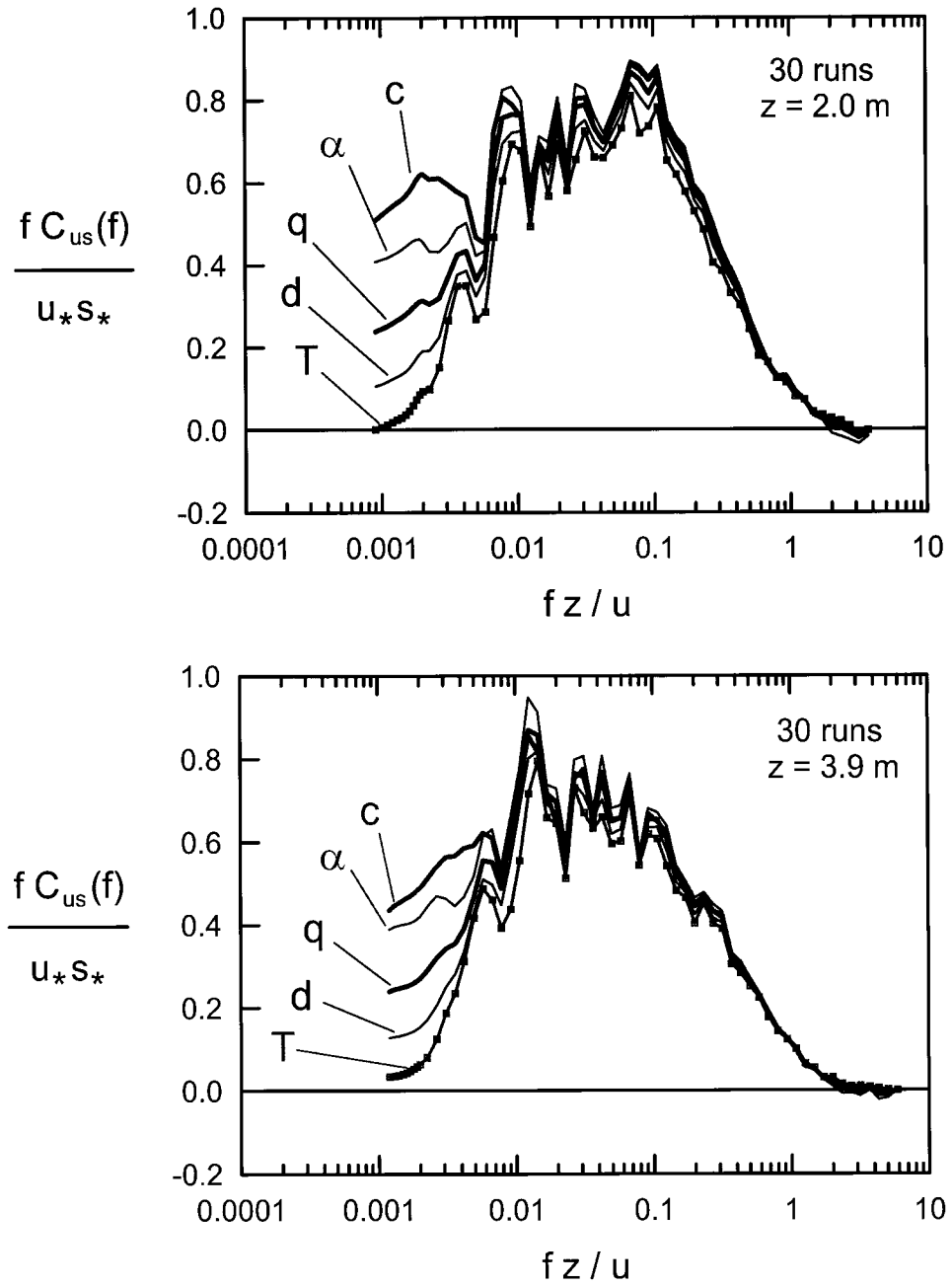

Figure 15. Cospectra of the horizontal wind, u, and various scalars (a) at 2.0 m, (b) at 3.9 m. The cospectra have all been normalized on the vertical flux measured at 2.0 m.

The scalar scale parameter in Equations (10) and (13) must also be replaced. The scaling s_* ($=-F_s/u_*$) is not suitable because s_* is related to the whole flux, not just the ILS component of it as required by Equation (13). We recall that the Kansas cospectrum had to be scaled down to fit the ILS component of our cospectrum (Figure 12). We require a scale capable of describing just the ILS component of flux.

We propose $\hat{s}_*$ as the correct scale for scalars in Equations (10) and (13), where $\hat{s}_*$ is defined by

$$\hat{s}_* = kz\frac{\partial \bar{s}}{\partial z}. \tag{14}$$

The von Kármán constant, k is included in this definition to ensure that $\hat{s}_* \rightarrow s_*$ as $v_* \rightarrow 0$. We note that this is an internal scale, determined by the scalar field accommodating to the velocity field and the boundary conditions; in this it is similar to u_*. The scale $\hat{s}_*$ is independent of height when the profile varies as the logarithm of height. This definition of $\hat{s}_*$ is the only one possible using first moments (i.e., not depending on the spectra themselves). It is consistent with the 'diffusive' property often attributed to ILS turbulence variance and also with the flux production terms in the turbulence budget equations being written as products with mean gradients (Stull, 1988). It is also consistent with our argument that the CS scalar fluctuations arise from distortions of the vertical scalar gradient.

Use of gradients to define $\hat{s}_*$ suggests that the accommodation of the CS and ILS components of the flux to a given v_* is via adjustment of the gradients; increased v_* would lead to a larger CS flux, and so smaller ILS flux and reduced gradient, maintaining a total eddy flux just equal to the source flux. The gradient will therefore shrink as the CS component of flux grows, so we expect eddy diffusivities to increase with increasing disturbance. In support of this deduction we note that eddy diffusivities at Warrawidgee were larger than those predicted by Monin–Obukhov similarity theory, which ignores disturbance (Laubach et al., 2000). For momentum the CS flux is zero and so cannot affect momentum diffusivities in a similar way. With minor correction, which we will not discuss here (but see Townsend, 1976), u_* remains the correct ILS velocity scale.

The final scale to consider is the scalar scale for the OLS spectral component. The OLS velocity scale is v_*. The search for a scalar scale is complicated by the fact that the OLS spectrum itself may have two or more parts; there may be scalar fluctuations embedded in the boundary layer whose origin is upwind surface heterogeneity; there may be fluctuations arising from CBL convective processes or entrainment; and there may be fluctuations arising from interaction with the lower boundary conditions. The last was prominent in our experiment. Indeed, we used this sensitivity as a distinguishing feature of the OLS component of scalar spectra and cospectra at Warrawidgee. This means that, for this component, there exists a dependency on $\mathrm{d}F_s/\mathrm{d}s$. However, $\mathrm{d}F_s/\mathrm{d}s$ does not bear a scalar dimension, so it cannot itself be the basis for a scalar scale. Its effect must be through dependence

on a dimensionless group, possibly $u_*^{-1}\ \mathrm{d}F_s/\mathrm{d}s$. The scalar scale for this OLS component seems to be $\hat{s}_*$ because this part of the OLS fluctuations depends on variations of scalar gradient in the surface layer. The convective scale $F_{s,0}/w_*$ is probably important for the convective component, and a scale characterizing spatial variability of the scalar concentration upwind probably characterizes a third component. Further speculation on these scales is not warranted.

It might be noted that the scheme developed above challenges Monin–Obukhov similarity theory when it is applied to the typical daytime situation of an unstable surface layer within a convective boundary layer. The similarity scale for the CS parts of scalar flux would then be $\sqrt{u_* w_*}\,\hat{s}_*$ where $w_* = \langle u_* \rangle (k)^{-1/3} (z_i/\langle L \rangle)^{1/3}$ and the angle brackets indicate that the average is over the whole generating area for the CBL-scale convection. The similarity scales for the ILS components of spectra would be u_* and $\hat{s}_*$, where $\hat{s}_*$, being an internal scale, already reflects buoyancy acting both locally and through the disturbing effects of OLS motions. The local effect of instability would be described by the parameter $z/\hat{L}$, where $\hat{s}_*$ has replaced s_* in the usual definition of the Obukhov length, thus $\hat{L} = u_*^2 T/kg(\hat{T}_* + 0.61\hat{q}_*)$. The gradient scale is appropriate here because buoyancy acts locally on density differences and so directly on the gradients. The ratio $\hat{s}_*/s_*$ is the dimensionless scalar gradient $\phi_h(z/\hat{L},\ z/\langle L \rangle)$, which Monin–Obukhov theory proposes should be a function of $z/\hat{L}$ only. The temperature gradient itself therefore does not obey Monin–Obukhov similarity. This means that any local effects that buoyancy has on velocity spectra or profiles will also depend on both $z/\hat{L}$ and $z_i/\langle L \rangle$. Unlike Monin–Obukhov theory, we do not predict $\phi_h \to 0$ as $z \to 0$ since the CS component of flux is independent of height. That $\hat{s}_*$ is the only universal scale for the ILS spectrum means that all quantities defined by properties of the inertial subrange will scale on $\hat{s}_*$ rather than s_*, and so will depend on both z/L and $z_i/\langle L \rangle$.

Our predictions of the importance of $z_i/\langle L \rangle$ when describing turbulence in the surface layer is consistent with the simulation studies of Khanna and Brasseur (1998) and the field results of Johansson et al. (1999).

6. Townsend's Hypothesis and the Disturbed Atmospheric Surface Layer

Our research programme has used Townsend's hypothesis as a fundamental idea, but in an extended form applied to scalars as well as to velocity components (McNaughton and Laubach, 1998). We now examine this extended hypothesis in the light of our spectral studies. Initially, our conceptual model assumed that spectra could be divided into OLS and ILS parts by some simple kind of decomposition operator. An example of this would be a simple filter that could discriminate high and low frequency components each side of a spectral gap. In fact, only our v spectrum displays such a gap. Our scalar spectra, in particular, showed no trace of such a feature. This led us to question Townsend's assessment that there was no interaction between 'active' and 'inactive' turbulence.

This created a problem. Our earlier theory represents the CS components of scalar fluxes as $(\overline{w'_p s'_a} + \overline{w'_a s'_p})$ and $(\overline{u'_p s'_a} + \overline{u'_a s'_p})$ (McNaughton and Laubach, 1998). It then sets these flux components to zero, arguing, in particular, that w'_p must be small near the ground because large eddies must be horizontal and, in general, that all covariances of active and inactive quantities are zero because their fluctuations have different origins and frequencies. Present results show that the OLS and ILS motions do interact, and we have argued that the result of this interaction is a CS part of each spectrum and cospectrum. We have argued, in particular, that the CS part of the scalar fluxes can be a substantial fraction of total vertical fluxes in disturbed conditions. How then are we to align our spectral division into OLS, CS and ILS parts with our earlier theory based on dividing fluctuations into active and inactive parts?

The answer appears to be straightforward. We simply classify all OLS components as passive and all CS and ILS components as active. We have argued that we can view the OLS variations in u and v as a varying wind profile superimposed on the steady wind profile, both maintaining a logarithmic shape. The OLS fluctuations in vertical velocity result from convergences in this horizontal field, but they are inactive because they are 90° out of phase with all CS scalar and velocity fluctuations. 'Fast' ILS turbulence processes maintain a continuous equilibrium with the 'slow OLS variations in the wind. These interpretations lead us to modify and extend Townsend's hypothesis itself (Townsend, 1961). Our OLS motions correspond to Townsend's conception of 'inactive' motions, which were said to swirl about the active eddies in a horizontal direction; we include a vertical component in these inactive motions, but maintain its inactivity by having it 90° out of phase with other fluctuations. Our ILS motions correspond to Townsend's active eddies, which he associated with fast accommodation of wall stress (Townsend, 1976). However, we find that there is an interaction between these two types of motion, and we find that the resulting CS motions are active in transport of both heat and momentum. The momentum transfered is, however, in random directions and has zero mean.

In summary, we classify OLS motions as inactive and attribute properties to them that are in accord with those proposed by Townsend (1961). We classify all CS and ILS components of turbulence as active, modifying Townsend's concept by including the product of the OLS and ILS interaction. When this is done Townsend's hypothesis is fully supported, as is its extension to scalars, as described by McNaughton and Laubach (1998).

7. Conclusions

We have given a comprehensive analysis of the velocity and scalar spectra observed in a disturbed surface layer at the base of an advective inversion formed over a

freely-transpiring rice paddy. In doing this we have been lead to propose a new structure for scalar spectra and cospectra.

We have proposed that scalar spectra and cospectra have three components, which we call inner-layer scaling (ILS), outer-layer scaling (OLS) and combined scaling (CS) components. These are classified according to their dependence on height and frequency. The ILS components scale on normalized frequency, fz/u and their amplitude is independent of height; the OLS components scale on fz/U_m (where U_m is the mixed-layer wind velocity) and their amplitudes vary with height; and the CS components are independent of frequency and of height. Of these components the CS component is new. In being independent of height and frequency, CS turbulence spectra observe the behaviour predicted for a 'mixed convection layer', as hypothesized by KY91. However, the velocity and scalar scales we find for these components do not match their predictions.

In our scheme the OLS motions are predominantly horizontal and reflect the action of the external disturbance. The OLS component of vertical motions is small but important. The ILS components of velocity consist of 'fast' shear-created turbulence in continuous equilibrium with the 'slow', horizontal OLS motions. The CS components of spectra arise from an interaction between the OLS vertical motions and the ILS fields of velocity and scalar. We have found that the scales originally proposed by Kader and Yaglom (1991) are not appropriate for our results and we have proposed new scales. We find that Townsend's hypothesis can be extended to scalars if we classify as 'active' any fluctuation associated with the ILS and CS components of spectra, and as 'inactive' all OLS components. With this done, our earlier work on the effects of unsteadiness on the ratios of scalar diffusivities (McNaughton and Laubach, 1998) remains valid.

The processes underlying the existence of OLS, ILS and CS components of turbulence do not appear to be limited to stable layers beneath convective ones, such as we have studied, and surface layers disturbed by topographically-induced turbulence. They should also apply to the unstable surface layer within a CBL, as is the normal daytime condition. This leads us to extend our results to ordinary daytime conditions in the surface layer. We predict that CBL convection disturbs the surface layer there also, so that inner-layer and outer-layer scales are important. That is, we propose that Monin–Obukhov scaling theory is incomplete for daytime conditions.

Note added in proof: This paper has been modified at proof stage (Sections 4.2.4 and 5) to include the interpretation that the CS parts of our scalar spectra may derive from by spaced large, localized flux events. This interpretation suggests a connection between OLS motions and the occurrence of coherent structures in the atmospheric surface layer. We plan to explore this connection in a later paper.

Acknowledgements

We thank Angelo Silvestro who allowed us to set up our equipment in his rice paddy at Warrawidgee and looked after us during our stay. We also thank the staff of CSIRO Land and Water for a great deal of logistical support in the field, particularly John Blackwell at Griffith and Peter Coppin and Greg Foster in Canberra. A substantial part of this work was carried out under contract CO 6539 with the Marsden Fund of New Zealand. The experimental work was conducted while the authors were employed by The Horticulture and Food Research Institute of New Zealand Ltd. Some of the interpretation was carried out under HortResearch Consultancy Contract 4776 to KGM.

References

Andreas, E. L.: 1987, 'Spectral Measurements in a Disturbed Boundary Layer over Snow', *J. Atmos. Sci.* **44**, 1912–1939.

Auble, D. L. and Meyers, T. P.: 1992, 'An Open Path, Fast Response Infrared Absorption Gas Analyzer for H_2O and CO_2', *Boundary-Layer Meteorol.* **59**, 243–256.

Bradshaw, P.: 1967, ' "Inactive" Motion and Pressure Fluctuations in Turbulent Boundary Layers', *J. Fluid Mech.* **30**, 241–258.

Carslaw, H. S. and Jaeger, J. C.: 1950, *Conduction of Heat in Solids*, Clarendon Press, Oxford, 386 pp.

de Bruin, H. A. R., Bink, N. J., and Kroon, L. J. M.: 1991, 'Fluxes in the Surface Layer under Advective Conditions', in T. J. Schmugge and J. André (eds.), *Land Surface Evaporation: Measurement and Parameterization*, Springer-Verlag, New York, pp. 157–169.

de Bruin, H. A. R., Kohsiek, W., and van den Hurk, B. J. J. M.: 1993, 'A Verification of Some Methods to Determine the Fluxes of Momentum, Sensible Heat and Water Vapour Using Standard Deviation and Structure Parameter of Scalar Meteorological Quantities', *Boundary-Layer Meteorol.* **63**, 231–257.

Haugen, D. A., Kaimal, J. C., and Bradley, E. F.: 1971, 'An Experimental Study of Reynolds Stress and Heat Flux in the Atmospheric Surface Layer', *Quart. J. Roy. Meteorol. Soc.* **97**, 168–180.

Högström, U.: 1990, 'Analysis of Turbulence Structure in the Surface Layer with a Modified Similarity Formulation for Near Neutral Conditions', *J. Atmos. Sci.* **47**, 1949–1972.

Johansson, C., Smedman, A.-S., Högström, U., Brasseur, J. G., and Khanna, S.: 1999, 'Critical Test of the Validity of Monin–Obukhov Similarity During Convective Conditions', *J. Atmos. Sci.*, submitted.

Kader, B. A. and Yaglom, A. M.: 1991, 'Spectra and Correlation Functions of Surface Layer Atmospheric Turbulence in Unstable Thermal Stratification', in O. Metais, and M. Lesieur (eds.), *Turbulence and Coherent Structures*, Kluwer Academic Publishers, Norwell, MA, pp. 388–412.

Kaimal, J. C. and Finnigan, J. J.: 1994, *Atmospheric Boundary Layer Flows*, Oxford University Press, New York, 289 pp.

Kaimal, J. C., Wyngaard, J. C., Izumi, Y., and Coté, O. R.: 1972, 'Spectral Characteristics of Surface-Layer Turbulence', *Quart. J. Roy. Meteorol. Soc.* **98**, 563–589.

Katul, G. and Chu, C.-R.: 1998, 'A Theoretical and Experimental Investigation of Energy-Containing Scales in the Dynamic Sublayer of Boundary-Layer Flows', *Boundary-Layer Meteorol.* **86**, 279–312.

Katul, G. G., Albertson, J. D., Cheng-I Hsieh, Conklin, P. S., Sigmon, J. T., Parlange, M. B., and Knoerr, K. R.: 1996, 'The "Inactive" Eddy Motion and the Large-Scale Turbulent Pressure Fluctuations in the Dynamic Sublayer', *J. Atmos. Sci.* **53**, 2512–2524.

Katul, G. G., Schieldge, J., Hsieh, C.- I., and Vidakovic, B.: 1998, 'Skin Temperature Perturbations Induced by Surface Layer Turbulence above a Grass Surface', *Water Resour. Res*. **34**, 1265–1274.

Khanna, S. and Brasseur, J. G.: 1977, 'Analysis of Monin–Obukhov Similarity from Large-Eddy Simulation', *J. Fluid Mech.* **345**, 251–286.

Lagouarde, J. P., Dubreton, S., Moreau, P., and Guyon, D.: 1997, 'Analyse de l'ergodicité de la température de surface sur des couverts forestiers à diverse résolutions', in G. Guyot and T. Phulpin (eds.), *Physical Measurements and Signatures in Remote Sensing*, Balkema, Rotterdam, pp. 303–310.

Lang, A. R. G., McNaughton, K. G., Chen Fazu, Bradley, E. F., and Ohtaki, E.: 1983a, 'Inequalities of Eddy Transfer Coefficients for Vertical Transport of Sensible and Latent Heats during Advective Inversions', *Boundary-Layer Meteorol.* **25**, 25–41.

Laubach, J. and McNaughton, K. G.: 1998, 'A Spectrum-Independent Procedure for Correcting Eddy Fluxes Measured with Separated Sensors', *Boundary-Layer Meteorol.* **89**, 445–467.

Laubach, J., McNaughton, K.G., and Wilson, J. D.: 2000, 'Heat and Water Vapour Diffusivities near the Base of a Disturbed Stable Internal Boundary Layer', *Boundary-Layer Meteorol*. **94**, 23–63.

McNaughton, K. G.: 1976, 'Evaporation and Advection I: Evaporation from Extensive Homogeneous Surfaces', *Quart. J. Roy. Meteorol. Soc.* **102**, 181–191.

McNaughton, K. G. and Laubach, J.: 1998, 'Unsteadiness as a Mechanism for Non-Equality of Eddy Diffusivities for Heat and Vapour near the Ground in an Advective Situation', *Boundary-Layer Meteorol.* **88**, 479–504.

Moore, C. J.: 1986, 'Frequency Response Corrections for Eddy Correlation Systems', *Boundary-Layer Meteorol.* **37**, 17–35.

Panofsky, H. A., Tennekes, H., Lenschow, D. H., and Wyngaard, J. C.: 1977, 'The Characteristics of Turbulent Velocity Components in the Surface Layer under Convective Conditions', *Boundary-Layer Meteorol.* **11**, 355–361.

Peltier, L. J., Wyngaard, J. C., Khanna, S., and Brasseur, J. G.: 1996, 'Spectra in the Unstable Surface Layer', *J. Atmos. Sci.* **53**, 49–61.

Phelps, G. T. and Pond, S.: 1971, 'Spectra of the Temperature and Humidity Fluctuations and of the Fluxes of Moisture and Sensible Heat in the Marine Boundary Layer', *J. Atmos. Sci.* **28**, 918–928.

Raupach, M. R., Antonia, R. A., and Rajagopalan, S.: 1991, 'Rough-Wall Turbulent Boundary Layers', *Appl. Mech. Rev.* **44**, 1–25.

Smeets, C. J. P. P., Duynkerke, P. G., and Vugts, H. F.: 1998, 'Turbulence Characteristics of the Stable Boundary Layer over a Mid-latitude Glacier. Part 1: A Combination of Katabatic and Large-Scale Forcing', *Boundary-Layer Meteorol*. **87**, 117–145.

Stull, R. B.: 1988, *An Introduction to Boundary Layer Meteorology*, Kluwer Academic Publishers, Dordrecht, 666 pp.

Townsend, A. A.: 1961, 'Equilibrium Layers and Wall Turbulence', *J. Fluid Mech.* **11**, 97–120.

Townsend, A. A.: 1976, *The Structure of Turbulent Shear Flow*, Cambridge University Press, Cambridge, U.K., 429 pp.

Wilczak, J. M.: 1984, 'Large-Scale Eddies in the Unstably Stratified Atmospheric Surface Layer. Part I: Velocity and Temperature Structure', *J. Atmos. Sci*. **41**, 3537–3550.

Zermeño-González, A. and Hipps, L. E.: 1997, 'Downwind Evolution of Surface Fluxes over a Vegetated Surface during Local Advection of Heat and Saturation Deficit', *J. Hydrol*. **192**, 189–210.